ijar
ISSN NO. 2320-5407

Journal Homepage: - www.journalijar.com

INTERNATIONAL JOURNAL OF ADVANCED RESEARCH (IJAR)

Article DOI: 10.21474/IJAR01/4551
DOI URL: http://dx.doi.org/10.21474/IJAR01/4551

RESEARCH ARTICLE

RAMAN, FT RAMAN AND FTIR SPECTRA OF MOLLUSCAN SHELLS.

R. Konwar[1] and G.D. Baruah[2].
1. Department of Physics, Tinsukia College, Tinsukia-786125, Tinsukia(Assam) India.
2. Centre for Laser & Optical Science, New Uchamati; DoomDooma-786151, Tinsukia(Assam) India.

……………………………………………………………………………………………………....

Manuscript Info

Manuscript History

Received: 20 April 2017
Final Accepted: 22 May 2017
Published: June 2017

Abstract

The present work reports the vibrational analyses of the FTIR and Raman spectra of few samples of molluscan shells procured locally for study. Raman spectra (including FT-Raman) show distinct band with highest intensity at 1085cm^{-1} which is presumably due to symmetric mode of vibration of the (CO_3^{2-}) group(ν_1), 702 cm^{-1} which is due to the in-plane bending mode and 206cm^{-1} and 274cm^{-1} which are characteristics of lattice vibrations of the crystal of calcium carbonate of aragonite type. The out of plane bending mode at 860cm^{-1} and designated as ν_3 is completely absent in the Raman spectra, but this band appears with strong intensity in the infrared spectra.

……………………………………………………………………………………………………....

Introduction:-

We are concerned in the present work with the FTIR and Raman spectra of the Molluscan shells. Spectral investigations of carbonate minerals contained in biological systems are very useful in solving the sedimental petrology problems of Mn^{2+} concentration and its distribution non-equivalent positions within the corresponding mineral structure, as produced by mineral crystallization and evolution. Structural investigations of biominerals such as Molluscan shells were studied extensively by ESR and other techniques[1-4]. It is also well known that molluscan shells have a high environmental significance and provide information on physiological events (duration of spawning period, growth etc.); moreover, they are clearly related with taxonomy and phylogeny. In the first extensive study of Molluscan shell structures Boggild[5] described and classified the main categories from mineralogical, crystallographic and micro structural characters. The most widespread structure was the aragonite crossed lamellar layer. However, distinctive micro structural and mineralogical features were noticed in different families. In subsequent decades studies were mainly directed towards bivalve shells[6-9]. FTIR spectroscopy is relatively rapid, simple and accurate for detecting calcium carbonate because calcium carbonate shows strong absorption peaks in infrared spectrum at 1430,875 and 712 cm^{-1}. These peaks are attributable to the vibration of carbon-oxygen double bond in the carbonate ion[10]. Especially the peak at 875 cm^{-1} is not overlapped with the peaks of other components, so it can be detected very easily and accurately in an unknown environment. However the main purpose of using FTIR will also be to identify the remaining organic components which are not easily found in Raman spectra. To analyse organic components in the samples of Molluscan shells which contain calcium carbonate as chief components (95 – 99.9%) and organic materials (5 – 0.1%)[11,12], the extraction with organic solvents can be a solution. But it is not always adoptable, and the choice of the appropriate solvent is important. Nacre is an extraordinary example a hierarchical biological nanocomposite and is found in the interior of many Molluscan shells[13,14]. Though nacre is composed of exceedingly weak constituent materials, its unique and highly organized

Corresponding Author:- R. Konwar.
Address:- Department of Physics, Tinsukia College, Tinsukia-786125, Tinsukia(Assam) India.

design at multiple length scales enables outstanding mechanical performance including an excellent combination of stiffness, strength, impact resistance and toughness[13-18]. The structure of nacre has been occasionally reviewed[19,20] and there is no doubt about its general structure. It is a composite material with a so called "brick-and-mortar" structure consisting of alternating layers of mineral tablets separated by thin layers of a biomacromolecular "glue". Nacre is composed of ~ 95wt% pseudo-hexagonal, polygonal, or rounded aragonite tablets which have dimensions of ~5 – 20 µm (plane with normal defined by the crystallographic c[100]-axis) and ~0.3 – 1.5 µm in thickness (vertically parallel to the c[001]- axis)[13,14]. The organic matrix of the nacre has been studied in a number of reports[21-34]. The intertablet polymer layer has a thickness that varies between ~30-300 nm with pores for mineral bridges to pass through, and intercrystalline proteins are present within the tablets themselves. It has become increasingly evident that knowledge of the fine details of the nanoscales properties will be critical to the success of such theoretical approaches in their attempt to understand macroscopical mechanical function and performance. Research in this direction is just beginning and FTIR, Raman study of the organic matrices of Molluscan shells be great help in understanding the physics of shell formations. In a Raman spectrum usually two sharp bands due to the vibrations of the carbonate ions are observed at 1085 cm^{-1}(symmetric stretching, ν_1) and705 cm^{-1} (in- plane bending, ν_4). The sharp bands at 207 cm^{-1} and 154 $cm^{-1}$are the characteristic of the aragonite structure[35]. Similarly the well known broadband on the FTIR spectrum is located at 3448cm^{-1} (OH and / or NH stretching modes of the organic matrix components). The 2800 – 3000 cm^{-1} range is characteristic of the C-H stretching modes and exhibits a small band at 2846 cm^{-1}. Protein complexes are demonstrated by the presence of intense bands at 1591 cm^{-1} (carboxylate groups coordinated asymmetric stretching band) and 1409 cm^{-1} (carboxylate symmetric stretching band). Smaller peaks detected at 1288, 1263, 921 and 850 $cm^{-1}$are characteristic of sulfate group, while the 1000 – 1150 cm^{-1} peaks correspond to the major polysaccharide absorption region. The presence of the bands at 1327 and 709 cm^{-1} indicate amide group absorption (amide III C-N stretching vibration and amide V/ VII respectively).

Both FTIR and Raman spectroscopy are valuable tools for characterizing the microstructure of biogenic and synthetic carbonates. These methods can also detect organic materials such as carotenoid pigment that is closely associated with the mineral matrix of biogenic carbonate. Variations in the positions and half widths of the Raman-active modes provide evidence of the presence of rotational disordering of the carbonate ion in carbonate. This rotational disorder is evident in calcite, but not in aragonite, owing to the presence of solid solution between Ca^{2+} and Mg^{2+} and the greater concentration of trace impurities in calcite. Fourier transform infrared spectroscopy analyses of mineral and organic matrix from the shell of the Molluscan Pinctade maxima were made by Balmain et. Al[36] who showed that amide, amine, and carboxylic acid groups in the organic matrix of whole nacreous layer, with the HCO_3^- groups possibly present at the organic-mineral interface. Raman investigation of pigmentary molecules in the Molluscan biogenic matrix was recently made by Barnard and Coworker[37] using the 514.5 nm laser line of Ar^+ laser. Shell species were chosen to obtain a variety of colour. The spectra obtained for the Molluscan pigments indicated that they are polyacetylenic in nature, and, from the spectral features it was deduced that the pigments were carotenoids with unmythylated polyacetylenic backbones of various conjugated lengths. Carotenoids are the dominant source of colour in nature and have been identified in many different body parts of marine invertebrates[38-41]. Molluses are not able to synthesize carotenoids themselves, as these are synthesized afresh only in plant kingdom. The exact chemical nature of the marine carotenoids of Molluscan origin is not known, but they are believed to be carotenoid derivatives[42,43]. Raman spectral features have been used extensively for probing the structural nature of carotenoids[44-46] and of the carotenoids' industrial counterparts, the polyacetylene derivatives[47-52]. Also the 514.5 nm laser wavelength falls within or close to the energy required for the electronic transition of most carotenoids or polyacetylene systems, resulting in the resonance Raman Effect that occurs for carotenoids. This feature makes Raman spectroscopy an ideal tool for in situ investigation of these pigments in the Molluscan matrix.

Experimental Methods:-

Fourier Transform Infrared Spectra:-

The samples of adult Unio were procured from the location – "Maguri Beel" of Dibru Saikhowa National Park, Tinsukia. The soft parts of the animal were removed and shells were rinsed with warm water, and then with cold water. The small pieces were ground into powder and the powdered samples were dried in an oven at 40^0C for one night. All spectra were recorded in KBr by a sophisticated computer controlled Perkin Elmer 2000 Fourier transform spectrometer (FTIR) from 4000 to 450 cm^{-1} with He-Ne laser as reference. The spectrometer was scanned at a resolution of 4cm^{-1} with steps of 1 cm^{-1} and the results are shown in Fig. 1.1 (a, b, c, d, f, g, h). Table 1.1 shows the prominent peaks observed along with the assignments indicating the origin of the peaks.

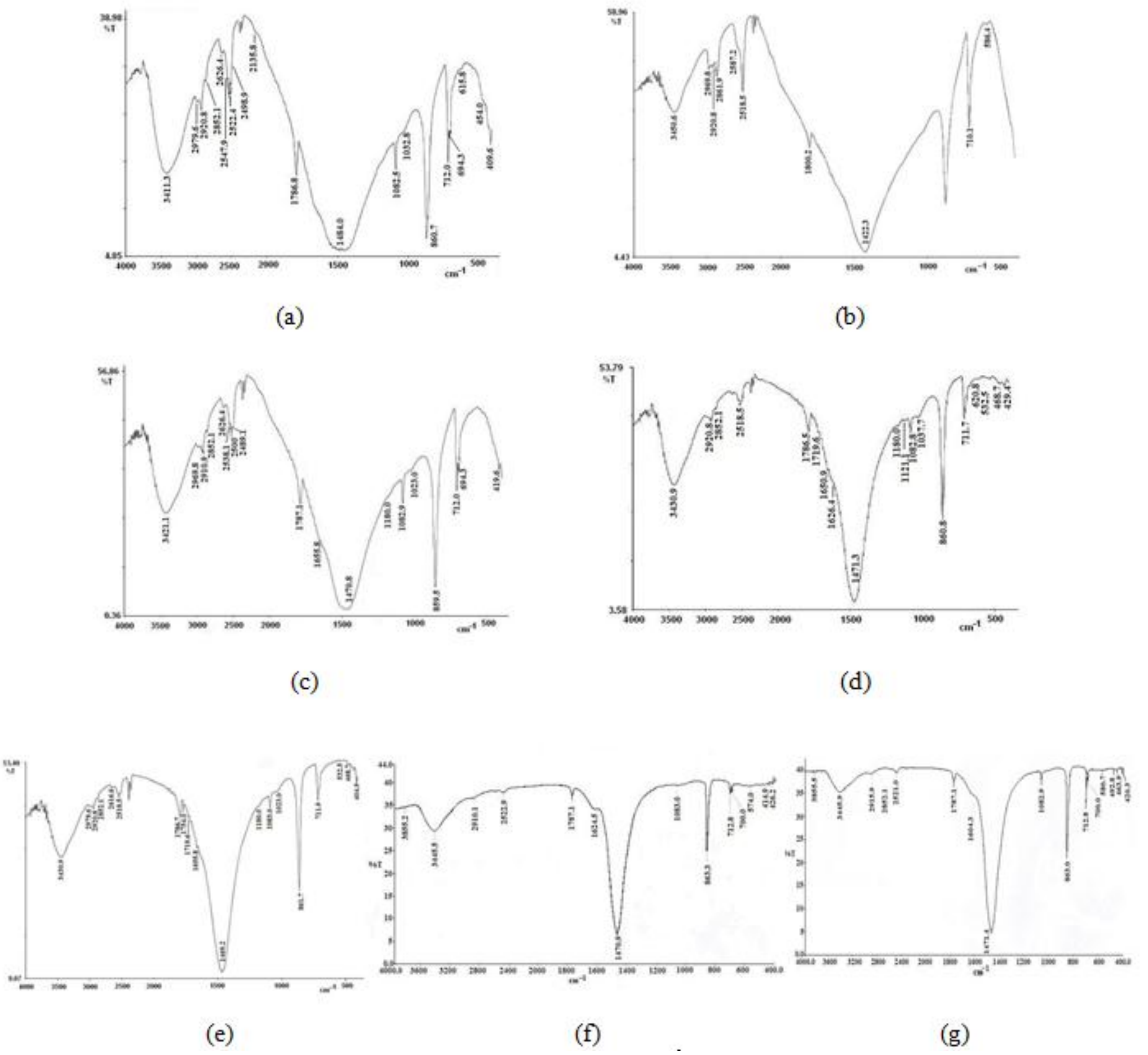

(a) (b) (c) (d) (e) (f) (g)

Fig 1.1:- (a, b, c, d, e, f, g)

FTIR Spectra of Molluscan Shells in powdered form (in KBR)

Table 1.1:- FTIR frequencies for Molluscan shells (cm^{-1}) and their assignments

Sample	a	b	c	d	e	f	g	Assignment
FREQUENCIES	3411(vs)	3451(vs)	3421(vs)	3431(vs)	3431(vs)	3445(s)	3446(s)	ν (OH)
	2979(ms)	2970(ms)	2970(s)					ν (NH)
	2921(s)	2921(ms)	2911(ms)	2921(ms)	2921(ms)	2910(vw)	2916(w)	ν (C-H)
	2852w)	2862(ms)	2852(w)				2852(w)	
	2626(w)		2626(w)					(HCO_2^{3-})
	2548(w)		2538(ms)					
	2522(s)	2518(vs)	2518 (ms)	2518(w)	2518(w)	2523(w)		
	2499(ms)		2489(ms)					
	1787(s)	1800(s)	1787(s)	1786(ms)	1787(s)	1787(ms)	1787(s)	ν (C=O)
			1655(w)		1656(w)			Amide-I
	1484(vs)	1422(vs)	1471(vs)	1471.3(vs)	1469(vs)	1471(s)	1471(vs)	ν_3
	1082(s)		1083(vs)	1083(s)	1083(ms)	1083(ms)	1083(ms)	ν_1

	1033(w)			1037(w)	1023(w)			
	861(vs)	869(vs)	859(s)	861(vs)	862(vs)	863(vs)		ν_2
	712(s)	710(vs)	712(vs)	712(s)	712(s)	713(s)	713(ms)	ν_4
	616(ms)		694(s)			700(ms)	700(ms)	Amide V
				621(w)				
		586(w)						
	454(w)			468(w)			464(w)	
	410(ms)		419(w)	429(w)	405(w)			

The relative intensities are shown in the parentheses: s= strong, vs = very strong, ms= medium strong, w= weak

ν_1 = symmetric stretching vibration of the carbonate ions

ν_2 = out – of – plane bending

ν_3 = CO_3^{--}(asymmetric)

ν_4 = in – plane – bending

From the data exhibited graphically in Fig 1.1, Table 1.1 has been prepared to exhibit the salient features in the FTIR spectra. There are few well known and prominent vibrational peaks which appear in the spectra and their interpretation are briefly described as follows. The strong and broad band located in the region 3411 to 3451 cm^{-1} is presumably due to the OH or NH stretching modes of the organic matrix components. The 2800 – 3000 cm^{-1} range is characteristic of the C-H stretching modes, and exhibits a group of frequencies. The group of frequencies in the range 2500 to 2626 cm^{-1} needs to be carefully interpreted as they do not appear under normal circumstances. It is reasonable to interpret them as originating from organic matrix (OH groups of carboxylic amino acids) and / or carbonate groups (HCO_2^{3-}) present in the mineral component. The strong peak located at 1787 cm^{-1} is due to the C=O groups of the carbonate ions. In fact there is no ambiguity in this assignment. The weak bands at 1655 cm^{-1} and 1656 cm^{-1} are considered as amide–I bands. Similarly another reasonably strong band at about 616 cm^{-1} is identified as amide-V band. In addition to these bands we are left with the well known strong bands at 1484 cm^{-1}, 1471 cm^{-1}, 1471.3 cm^{-1}, 1469 cm^{-1} and 1422 cm^{-1}. These bands are known as ν_3 band originating from asymmetric $CO_3^{- -}$ stretching mode. It may be noted that this is the strongest band in the IR spectra with largest value of half width at half maxima (HWHM). The other bands at about 1083 1422 cm^{-1} are known as the ν_1 and ν_3 bands which originate from the symmetric and asymmetric stretching vibrations respectively of the carbonate ions. The band at 861 cm^{-1} is known as ν_2 band and is the characteristic band of out of plane banding vibration. The band at 713cm^{-1} is also very strong and is due to in-plane-bending mode and is known as ν_4 band. The bands designated as ν_1, ν_2, ν_3 and ν_4 are well known absorption bands due to calcium carbonate. It is worthwhile to note that the relative intensities of these bands vary in different samples. The band at 861 cm^{-1}(ν_2) is reasonably strong in sample 1 while the band at 1083 cm^{-1}(ν_1) is completely absent in sample 2. As we have described so far calcium carbonate in the body of the shell can be detected very rapidly and easily by FTIR, paying attention to the absorption peaks at 1484 cm^{-1}(ν_3), 1082 cm^{-1} (ν_1), 861 cm^{-1}(ν_2) and 712 cm^{-1}(ν_4). These peaks are not overlapped with the peaks of other components, so they can be identified very accurately. However, our main purpose to use FTIR was to identify the remaining organic components in the samples. The organic components may be easily identified in the region of wave numbers of 2000 – 4000 cm^{-1}. However as shown in Fig 5.1 the absorption peak of calcium carbonate at 1484 cm^{-1} is sufficiently broad and this is possibly due to the overlapping of the absorption peaks of binding media.

Raman Spectra:-

The Raman spectra of the powdered samples of molluscan shells are recorded with the help of a Raman Spectrometer (Model Jobin Yvon 3000 V) with Triax monochromator. He-Cd laser line at 442 nm (cw) is used as the exciting radiation. The FT-Raman spectra of the powdered samples are recorded with a Bruker Spectrometer (model IFS 120 HR) equipped with an integrated FRA 106 Raman module. The 1064 nm radiation from Nd: YAG laser with an output of about 150 mW is used for excitation. The spectral range of interest is 0 – 4000 cm^{-1}. Fig 1.2(a,b,c) shows the FT-Raman spectra of three samples of molluscan shells and Fig 1.3(a,b,c,d,e) shows the Raman spectra of five samples excited by He – Cd laser line at 442 nm with maximum power of 300 mW. The spectral range considered in this case is 0-200 cm^{-1}.

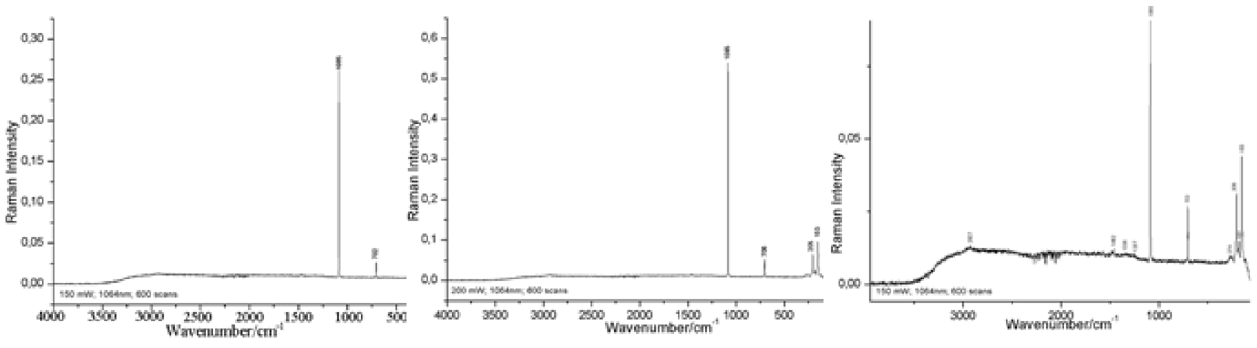

(a) (b) (c)

Fig 1.2:- (a, b, c) FT-Raman spectra 0f molluscan shells.

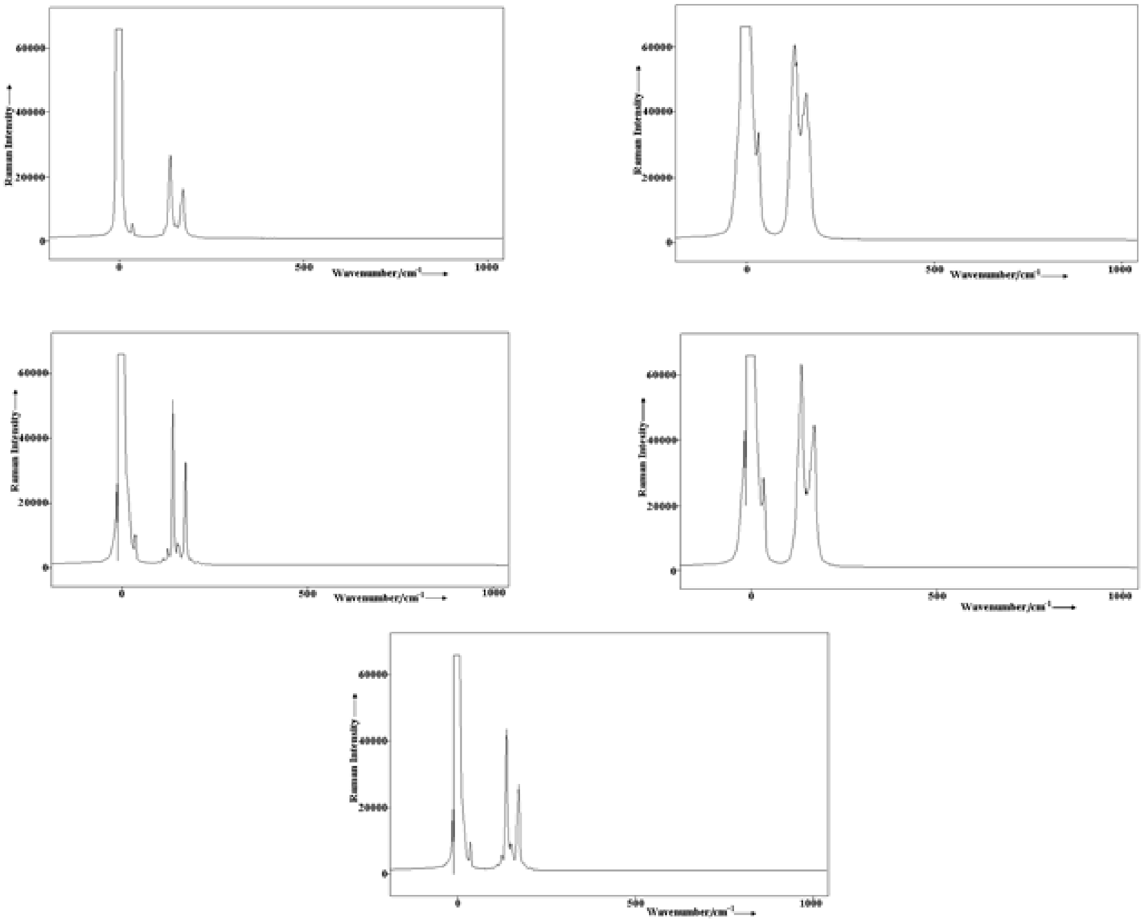

Fig 1.3:- (a, b, c, d, e), Raman spectra of five samples of molluscan shells
in the range 0 – 200 cm^{-1}

Table 1.2:- FT-Raman frequencies of Molluscan Shells (cm^{-1})

Sample a	Sample b	Sample c	Assignment
		2927 (w)	– CH Stretching
		1462 (w)	– CO_3^{2-} (ν_3)
		1336 (w)	–
		1257 (w)	–
1085 (vvs)	1085 (vvs)	1085 (vvs)	– CO_3^{2-} (ν_1)
702 (vs)	706 (vs)	702 (vs)	ν_4
		274 (ms)	Lattice
206 (s)	205 (s)	206(vs)	Lattice
		181(ms)	Lattice
153 (s)	153 (s)	153 (vs)	Lattice

vvs = very very strong; vs = very strong; ms = medium strong; w = weak.

Table 1.3:- Raman frequencies in molluscan shells observed below 200 cm^{-1}.

Sample					Analysis
a	b	c	d	e	
37 (s)	40(vs)	40 (s)	40 (ms)	40(s)	Lattice
113 (w)					Lattice
			93 (w)		Lattice
			113 (w)		Lattice
126 (w)	127 (vs)		126 (ms)		Lattice
139 (vs)		133 (vs)	137 (vs)	139 (vs)	Lattice
145 (ms)	147 (w)		147 (ms)		Lattice
			149 (ms)		Lattice
165 (vs)	166 (s)	158 (s)	166 (s)	173(s)	Lattice
184 (w)			186 (w)		Lattice
			203 (w)		Lattice

Intensities are given in the parenthesis
s = strong; w = weak; ms = medium strong; vs = very strong.

The FT-Raman spectra of the molluscan shells exhibit only three prominent bands. They are at 1462 cm^{-1} with extremely weak intensities which is due to antisymmetric stretching mode of CO_3^{2-} group (ν_3). This weak band is completely absent in the spectra of the remaining two samples. The band at 1085 cm^{-1} is due to the symmetric mode vibration of the CO_3^{2-} group (ν_1). Another strong band at 702 cm^{-1} (ν_4) is observed with very strong intensities in the Raman spectra. This band at 702 cm^{-1} is due to the in-plane-bending modes of carbonate ions. It may be noted here that the out of plane bending mode of vibration at 860 $cm^{-1}$and designated as ν_2 is completely absent in the Raman spectra whereas this band appears with strong intensity in the FTIR spectra. This is presumably due to the usual selection rule. The band due to ν_2 is not Raman active. The inorganic compound of molluscan shells primarily consists of $CaCO_3$. $CaCO_3$ can exist as three polymorphs; calcite, aragonite and vaterite. It is possible to distinguish between the three phases by Raman spectroscopy, as each of them has unique, non-overlapping peaks. Vaterite has bands at 738 cm^{-1} and 750 cm^{-1}, aragonite a doublet at 700 cm^{-1} and 705 cm^{-1} and a calcite band at 711 cm^{-1}. From the consideration set forth here aragonite is the only form observed in the present case. The most intense band for all the three phases occurs at ~ 1086cm^{-1}, which is assigned to the symmetric CO_3^{2-} stretching mode. From this frequency it is not possible to distinguish between the three phases.

The medium intensity bands in the region of 100 – 300 cm^{-1} of the Raman spectra arise from the translational and rotational modes of lattice vibrations. Lattice vibrations of aragonite at 206 cm^{-1} and 274 cm^{-1} are clearly observed in the Raman spectra. The Raman bands observed below 200 cm^{-1}, as shown in Fig 1.3 and Table 1.3 indicate few features which have not been reported until now. Vibrational frequencies characteristics of the lattice modes are observed in large numbers. As for example ten frequencies are measured in sample d. In FT-Raman only three lattice vibrational modes have been identified. A proper identification of these low frequency modes will require a detailed investigation of the organic macromolecules in the growth of biogenic crystals, biogenic crystals differs in some aspects from its geological counterparts.

Summary and Conclusion:-

The present works reports the vibrational analyses of the FTIR and Raman peaks observed in the samples of the molluscan shell. Raman spectra (including FT-Raman) show distinct peaks at 1085 cm^{-1} which is due to symmetric mode of vibration of the CO_3^{2-} group (ν_1), 702 cm^{-1} (ν_4) which is due to the in-plane-bending mode and 206 cm^{-1} and 274 cm^{-1} which are characteristic of lattice vibrations of the crystals of calcium carbonate of aragonite type. The out-of-plane bending mode at 860 cm^{-1} and designated as ν_2 is completely absent in the Raman spectra, but this band appears with strong intensity in the infrared spectra. ν_1, ν_2 ν_3 and ν_4 bands are considered as fingerprint bands of calcium carbonate molecules. There are two common forms of calcium carbonate, aragonite and calcite. They differ in their crystal shape, yet their chemical formula is the same. Whether calcium carbonate becomes aragonite or calcite depends on the "seed crystals" growth pattern. The molluscan shells in the present work are composed of the aragonite form of calcium carbonate. Proteins and amino acids secreted by the polyp play role in the growth of the crystals of aragonite and probably determine whether aragonite or calcite forms. Raman and FTIR spectroscopy are valuable tools for characterizing the microstructure of biogenic and synthetic carbonates. This method can also detect organic materials that are closely associated with the mineral matrix of biogenic carbonate

Acknowledgement:-

The author (Konwar. R) is grateful to UGC for award of a minor research project (MRP). No: F.5-390/2014-15/(MRP/NERO) dated 24-03-2015. The author is also grateful to Prof W. Kieffer of University Wurzburg Institute for Physikalische Chemie, Am Hubland D-97074, Wurzburg Germany for working out the Raman spectra of the samples in his laboratory.

References:-

1. Y. Nagaraja Naidu, J. L. Rao, and S.V.J. Lakshman, *Polyhedra*, **11**, 663 (1992).
2. L. Douifi, J. Raffi and M. Prost, *J. Chim. Phys (Fr)* **96**, 188 (1999).
3. V.N. Laslo and L. Brecevic, *Phys. Chem. Chem. Phys*, **1**, 3697 (1999).
4. K.V. Narasimhulu and J. Lakshmana Rao, *Spectrochin. Acta (A)*, **56**, 1345 (2000).
5. O.B. Boggild, Kong. Dsk. Vidensk Selsk. Skr, *Nature, Math. Afd.* **9 Π 2**, 230-326 (1930).
6. J.D. Taylor, W.J. Kennedy and A Hall Bull. Br. Mus. *Natt. Hist. Zool.* **3**, 1-125 (1969).
7. I. Kobayashi; *Am. Zool*. **9**, 663-672 (1969).
8. I. Kobayashi; Various patterns of Biomineralization and its phylogenetic significances in bivalve mollusks. In: Omori, M. Watabe, N (eds). The mechanisms of Biomineralization in Animals and Plants, Tokai University Press, Tokyo., pp 145-155 (1980).
9. I. Kobayashi and J. Akai; *J. Geol. Soc*. Japan. **100**, 177-180 (1994).
10. W.B. White, "The carbonate minerals" In the Infrared Spectra of Minerals (V.C. Farmer, ed) 1974, pp 227-284, Mineralogical Society, London.
11. P. E. Hare and P.H. Abelson; Amino acid composition of some calcified proteins, Carnegie Institution Washington Year book, **64,** 223-232 (1965).
12. L.P.M.Timmermanns; Netherlands. *Journal of Zoology*, **19**, 417-523 (1969).
13. A.P. Jackson, J.F.V. Vincent and R.M. Turner, Proc. *R. Soc. London B. Bio. Sci.* **234**, 415 (1988).
14. S. Weiner and L. Addadi; *J. Mater. Chem*, **7,** 689 (1997).
15. R.Z. Wang, Z. Suo, A.G. Evans, N. Yao, and I.A. Aksay, *J. Mater. Research* **16**, 2485 (2001).
16. R. Menig, M.H. Meyers, M.A. Meyers and K.S. Vecchio, *Acta Mater*, **48**, 2383 (2000).
17. A.P. Jackson, J.F.V. Vincent and R.M. Turner; *J. Mater. Sci*., **25**, 3173 (1990).
18. J.D. Currey; *Proc. R. Soc. London B Bid Sci*, **196** (1125), 443 (1977).
19. H.K. Erban, *Biomineralization* **7**, 14 (1974).
20. J.D. Taylor, W.J. Kennedy and A. Hall Bull. Brit. Museum. Natural History Zool (Suppl. 3) **1**, (1969).
21. X. Xhen, A.M. Belcher, P.K. Hansma, G.D. Stucky and D.E. Morse; *J. Bio. Chem*. **272**, 32472 (1997).
22. Y. Zhang, L. Xie, Q. Meng, T. Jian g, R. Pu, L. Chen and R. Zhang; *Biochem. Physiol. Part B* **135**, 565 (2003).
23. S. Blank, M. Arnold, S. Khoshnavaz, L. Treecani, M. Kuntz, K. Mann, G. Grathwohi and M. Fritz; *J. Microsc.* **212**, 280 (2003).
24. F. Song, A. K. Soh, and Y.L. Bai; *Biominerals* **24**, 3623 (2003).
25. F. Song, X. H. Zhang and Y.L. Bai; *J. Mater. Res.* **17**, 1567 (2002).
26. B.A. Wustman, D.E. Morse and J. S. Evans; Langmuir, 18, 9901 (2002).
27. S. Weiner and W. Traub Philos. *Trans. R. Soc. London, Series B. Biol. Sci*. **304**, 425 (1984).
28. I. W. Weiss, S. Kaufmann, K. Manm, and M. Fritz, *Biochem. Biophys. Res. Commun*. **267**, 17 (2000).

29. I.M. Weiss, C. Renner, M.G. Strigl and M. Fritz; *Chem. Mater* **14**, 3252 (2002).
30. L. Pereira- Mouries, M. Almeida, C. Ribeiro, J. Peduzzi; M.J. Barthelemy, C. Milet, and E. Lopez *Eur. J. Biochem*. **269**, 4994 (2002).
31. L. Bedouet, M.J. Schuller, F. Marin, C. Milet, E. Lopez and M. Giraud; *Comp. Biochem. Physiol. Part B, Biochem Mol. Bio*. **128**, 389 (2001).
32. C. E. Brown and H. Tang; *Comp. Biochem. Physiol. Part A; Phys*. **115A**, 269 (1996).
33. S. Weiner, Y Talmon, and W. Traub; *Int. J. Biol. Macromol*, **5**, 325 (1983).
34. S. Weiner and W. Traub; *FEBS Letts* **111**, 311 (1980).
35. C.G. Kontoyannis and N.V. Vagenas; *Analyst* **125**, 251 (2000).
36. J. Balmain, B. Hannoyer and E. Lopez; *Applied Biomaterials*, **48**, 749-754 (1999).
37. W. barnard and D. de Wall, *J. Raman Spectry*, **37**, 342-352 (2006).
38. D.L. Fox. Chapter 8; Pigmentation of Mollusces: In Physiology of Mollusca, Vol 2 (1st ed), Wilber K.M., Yonge C. M.(eds), Academic Press,New York (1966).
39. J. Hudon; *Biotechol. Adv*. **12**, 49 (1994).
40. D.F. Cheesman, W.L. Lee, and P.F. Zagalsky, *Biol. Rev*. **42**, 132 (1967).
41. D. L. Fox: Animal Bischrome and Structural colors: Cambridge University Press: Cambridge, UK (1953).
42. J.C. Merlin and M.L. Dete-Dubois, *Bull. Soc. Zool. Fr*. **108**,289 (1983).
43. J.C.Merlin; *Pure Appl. Chem*. **57**, 785 (1985).
44. R.J.H. Clark, N.R. D'Urso and P.F. Zagalsky; *J. Am. Chem. Soc*. **102**, 6693 (1980).
45. R.J. Weesie, J.C. Merlin, H.J.M. We Groot, G. Britton, J. Lugtenburg, F.J.H.M. Jansen, and J.P. Cornard; *Biospectroscopy* **5**, 358 (1999).
46. J.C. Mertin; *J. Raman Spectrosc*. **18**, 519 (1987).
47. H. Kuzmany; *Phys. Sta. Sol*. **97B**, 521 (1980).
48. H.E. Schaffer, R.R. Chance, R.J. Sibey, K. Knoll, R. R. Schrock; *J. Chem. Phys*. **94**, 4161 (1991).
49. H. Takeuchi, Y. Furukawa, I. Harada, and H. J. Shirakawa; *J. Chem. Phys*. **80**, 2925 (1984).
50. M.A. Schen, J.C. W. Chien, E. Perrin, S. Lefrant, and E. Mulazzi; *J. Chem. Phys*. **89**, 7615 (1988).
51. G. Zerbi, C. Castiglioni and M. Gussani; *Synth. Met*. **43**, 3407 (1991).
52. M. Gussani, C. Castiglioni and G. Zerbi; *Synth. Met*. **28**, D375 (1989).

Journal Homepage: -www.journalijar.com

INTERNATIONAL JOURNAL OF ADVANCED RESEARCH (IJAR)

ISSN NO. 2320-5407

Article DOI:10.21474/IJAR01/11306
DOI URL: http://dx.doi.org/10.21474/IJAR01/11306

RESEARCH ARTICLE

ON THE NATURE OF LASER INDUCED FLUORESCENCE, SEM AND IRIDESCENT PATTERNS OF MOLLUSCAN SHELLS

R. Konwar[1], B. Gogoi[1], J. Saikia[2], Mitali Konwar[3] and G.D Baruah[4]

1. Department of Physics, Tinsukia College, Tinsukia-786125(India).
2. Department of Physics, J B College, Jorhat- 785001(India).
3. Principal, Moran College, Moran- 785670(India).
4. Centre for Laser & Optical Science, New Uchamati, DoomDooma- 786151.

……………………………………………………………………………………………………....

Manuscript Info

……………………….

Manuscript History
Received: 10 May 2020
Final Accepted: 15 June 2020
Published: July 2020

Key words:-
Molluscan Shell, Iridescence, LIF, SEM

Abstract

………………………………………………………………………

In the present work we report the Laser Induced Fluorescence (LIF), SEM and Iridescent Patterns of molluscan Shells. The intensity distribution patterns of different iridescent patterns are worked out with the help of software (Image J). The iridescent colours of shells are ascribed to diffraction and also due to laminated structure. Laser induced fluorescence spectra are recorded for a specimen in a organic solvent, using blue, green and red diode laser. Nine fluorescence peaks at 470, 450-600, 680, 718, 720, 734, 756, 820 and 840 nm are observed and their assignments have been proposed. The SEM patterns of a powered specimen are analysed.

……………………………………………………………………………………………………....

Introduction:-

Molluscan shells have been the subject of study among research workers during last many decades for interesting physical phenomena exhibited by these objects. The materials of the shells present different appearances in different cases. It is also well known that the molluscan shells have high environmental significance and provide information on physiological events such as the duration of spawning period, growth etc. Moreover they are clearly related to taxonomy and phylogeny. In an extensive study of Molluscan shell structures Boggild [1] described and classified the main categories from mineralogical, crystallographic and micro-structural characters. The most widespread structure was the aragonite crossed lamellar layer. However, distinctive micro structural and mineralogical features were noticed in different families. In subsequent periods studies were mainly directed towards bivalve shells [2-5]. Several decades earlier Raman and coworkers devoted much attention to the iridescent substances called the mother-of-pearl and investigated experimentally various optical properties including iridescent patterns [6-10]. It is generally estimated that the shell of a molluscan built out of calcium carbonate has 3000 times higher fracture resistance than crystal of calcium carbonate. In the present work we would like to critically examine Raman's work specifically in connection with the iridescent patterns exhibited by the shells. Recently, Konwar [10] and Konwar et.al. [11] have investigated experimentally various optical and spectroscopic properties of few molluscan shells. They have also recorded laser induced fluorescence of few shells in their natural form in a classical spectrograph using green Ar ion laser (60mW). The spectra recorded by the workers consist of a diffuse and broad band in the red yellow sector of the spectrum. It is worthy of remarks here that, in general, a sample of Molluscan shell contains calcium carbonate or calcite. Calcite is by far the more common in nature as compared to aragonite. These two forms, calcite and aragonite are chemically the same but physically different. Mother-of-pearl consists of chalk in the rarer from of aragonite, but as numerous crystals. These are imbedded in a horny substance forming layers approximately parallel to the surface of the shell. According to Raman [9] there may be eight thousand to twelve

Corresponding Author:- R. Konwar
Address**:-** Department of Physics, Tinsukia College, Tinsukia-786125(India).

thousand such layers per centimeter of thickness of the mother-of-pearl. We note here that the fluorescence band recorded earlier [11] on a classical spectrograph has its origin in the organic components in the sample of Molluscan shells (using organic solvents) have been estimated [12, 13] and it was seen that the chief components are the calcium carbonate (95 – 99.9%) and organic materials (5 – 0.1%). In the present work we report the laser induced fluorescence spectra of organic solvent extracts of molluscan shells excited with the help of blue, green and red diode lasers. The spectra have been recorded with the help of a sophisticated mini spectrometer. The fluorescence is presumably originating from the organic components in the molluscan shells. As may be inferred from the spectra described in section 3, many new features are present in the laser induced fluorescence spectra not reported in any earlier works. In spite of the extensive works done during several decades on various aspects of molluscan shells, the emergence of the field of nanoscience has greatly influenced the field of biomineralization. In the present work we have also reported the scanning electron microscopic (SEM) patterns for a molluscan shell sample in a powdered form in order to find a possible correlation with the iridescence colours.

Iridescence patterns of molluscan shells: What they are?

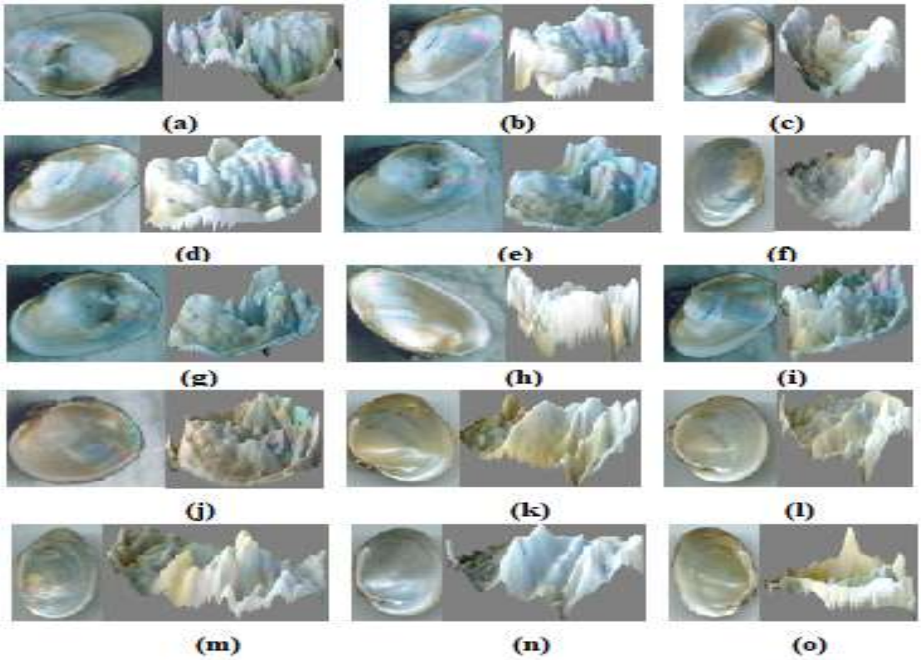

Fig: 1 Iridescence pattern of molluscan shells and their three dimensional intensity distribution patterns.

In some molluscan shells the coloured patterns, known as the iridescence patterns, are usually seen under normal condition of illumination. The iridescence colours of the shells have been usually ascribed to either interference or diffraction. Though the diffraction component is well established to account for the multicoloured iridescent patterns in shells the origin of the change in body colour in the case of pearl has not been fully established. Lord Rayleigh (following up some of his father's work) also was interested in iridescent colours of and optical structure producing it and one of his papers is devoted to the iridescent of beetles [14]. Similarly Ramdas [15] had investigated feeble iridescence from potassium chloride crystal. Potassium chloride belongs to the monoclinic class of crystal and in its natural occurrence takes the form of flat plates containing many twins. When the crystal plate is held so as to reflect light obliquely and is turned around in its own plane, colours alternately appear and disappear twice in its complete revolution. The spectral characteristic of the reflected light also varies with the angle of incidence. All the effects are associated with stratified media. Raman picked up the topic of stratified media and studied various specimens of natural origin for study. His study of the plumage of birds is the first of a series of publication, soon followed by two papers on iridescent shells [6,7]. In a recent work one author has described [16] how butterfly wings involve nano particles and systems containing photonic band gap. The work described by the author apparently needed more evidences to establish these facts.

We reproduce some examples of the molluscan shells under illumination by a broad band light of a scanner connected to a computer, as shown in Fig: 1(a, b, c, ……………..). We have also used the software (image J) to measure the three dimensional intensity patterns of the iridescent molluscan shells. It may be noted that the 3-D intensity distribution patterns are actually the manifestations of the optical properties associated with the alternate layers of conchin and aragonite crystal layers in different specimens. It is worthy of remark here that conchins are organic substances which are primarily proteins. Inner layers of calcium carbonate interface with a network of conchin and are impregnated with a variety of mineral salts. The calcium is usually in the form of calcite crystals in marine species and aragonite in terrestrial species but mixture of crystal types do occur. A close examination of the intensity distribution patterns show several peaks on the background and they are actually related to the conchin layers intersected with the surface of the shell and their configuration depends upon the curvature of the intersecting surfaces and the angle at which they meet. We thus find that method of three dimensional intensity patterns give qualitative information about the nature of iridescent pattern.

Laser induced fluorescence spectra of molluscan shells:

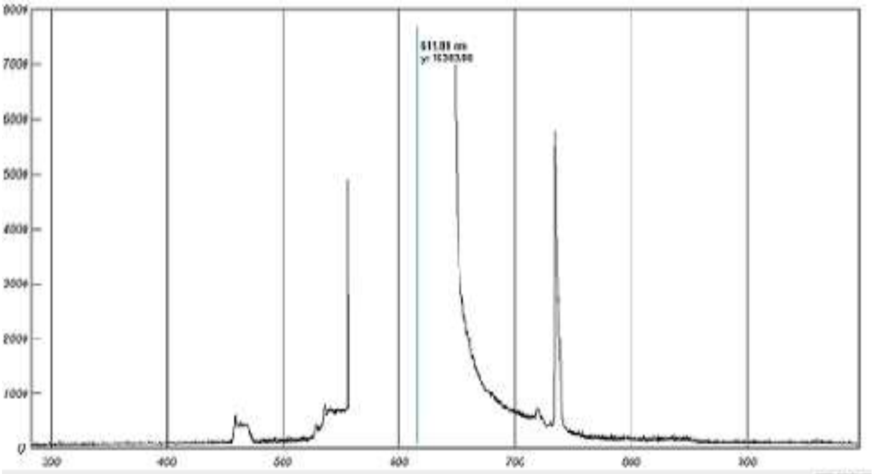

Fig: 4 Laser induced fluorescence spectrum of molluscan shell excited with the help of a red diode laser (~650nm, 20mW)

LIF of different molluscan shells are not in order and one of the LIF has no captions.

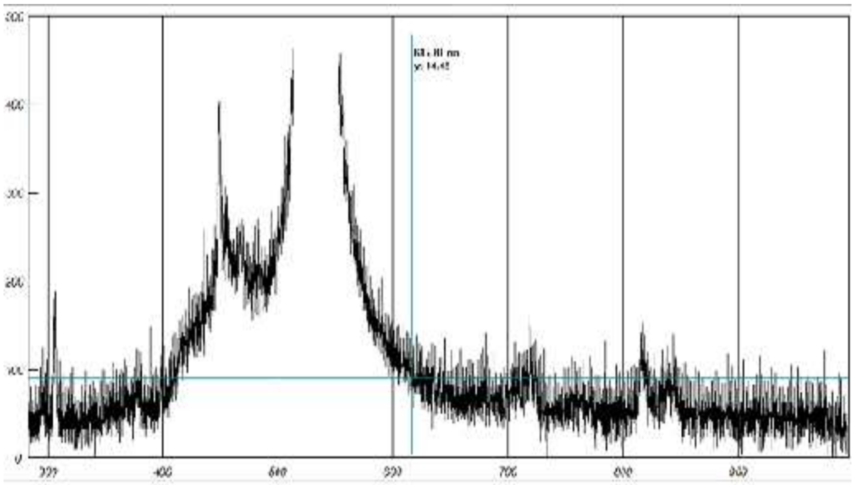

Fig: 3 Laser induced fluorescence spectrum of the liquid extract of molluscan shell excited with the help of green diode laser (~540nm, 30mW)

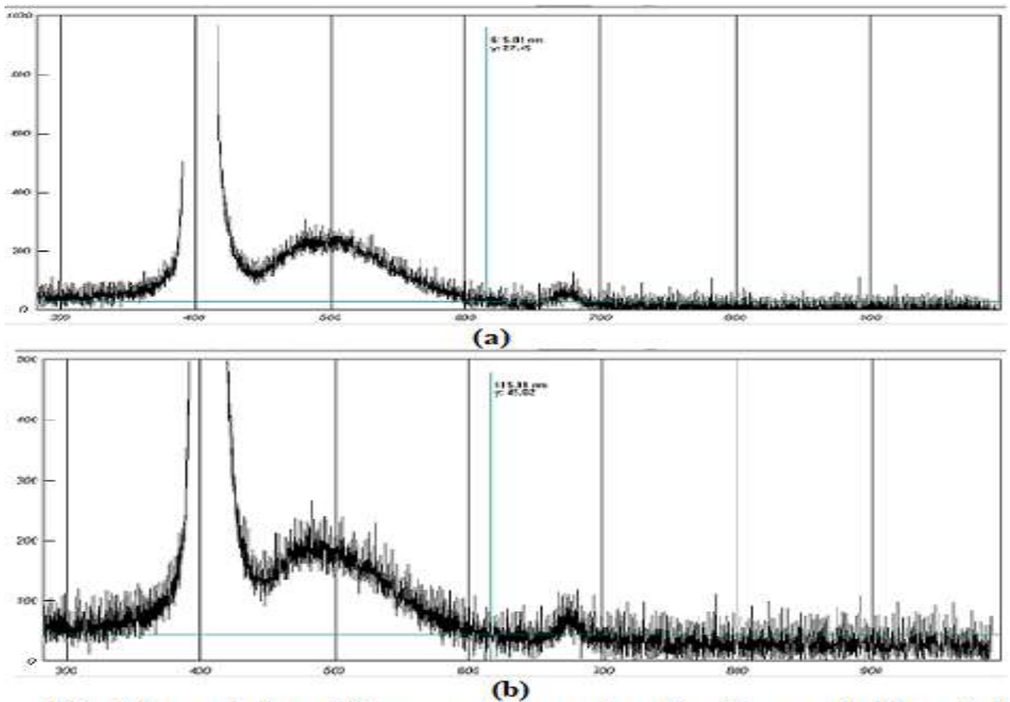

Fig: 2 Laser induced fluorescence spectra of molluscan shell excited by blue diode laser (~450nm, 10mW)

In the present section we discuss the laser induced fluorescence (LIF) of molluscan shell sample in an organic solvent. In the usual procedure immersion of the finely grinded powder of the shells in a glass vessel containing a suitable organic solvent (ethyl alcohol) enables the organic components of the molluscan shell responsible for their fluorescence to be quickly extracted. The extract may then be transferred to an observation curette of suitable length which is held against a brilliant radiation originating from a diode laser source. In the present case we have used diode lasers of three different colours red (~650nm, 20mW), green (~540nm, 30mW) and blue (~ 450nm, 10mW). The curette with the liquid sample is held in front of the opening end of the optical fiber connected to a mini USB spectrometer is connected to a laptop where the necessary software is installed for recording the spectra. Fig:2 (a, b) shows the spectra of the liquid extract of molluscan shell excited by blue laser. Fig:3 shows the laser induced fluorescence spectrum of the liquid extract of molluscan shell excited with the help of a green diode laser (~540 nm, 30mW) It is worthy of remark here that the fluorescence peaks lying below 500nm are spurious peaks present in the source itself. Similarly Fig: 4 exhibits the laser induced fluorescence spectrum of molluscan shell excited with the help of a red diode laser (~650nm, 20mW).

We now proceed to sum up the results which have emerged in this section. We first show the LIF peaks of the molluscan shell excited by three different lasers in the visible sector of the spectrum in Table: 1. The molluscan shells have been procured from the Maguri Bill (Wet land, saturated area of land) near Dibru Saikhowa National Park of Tinsukia district, Assam (India). It is quite significant to note that this area of land contains molluscan shells in abundance. We may also add here that such wetlands cover 5—10% of Earth's terrestrial surface [17]. Thus the present work on LIF of molluscan shell samples presumably bears significance in connection with any environment.

Table 1:- Laser induced fluorescence spectra of molluscan shells in the range 450- 1000 nm excited by blue, green and red diode lasers.

Wavelength (nm)	Relative intensity	Exciting Radiation (nm)	Assignments'
470	s	430	ν_1 (N_2 2^{nd} +ve)
450-600	s (broad)	430	ν_2
680	s	430	ν_3(N_2 1^{nd} +ve)
718	vw	650	ν_4 (CaO)
720	w	540	ν_4 (CaO)

734	vvs	650	ν_5(CaO)
756	vw	540	ν_6
820	ms	540	ν_7 (CaO)
840	ms	540	ν_8

s = strong, ms = medium strong, vvs = very very strong, w = weak and vw =very weak

As may be inferred from Table:1, we have identified eight fundamental band systems in the LIF spectra of the molluscan samples. The bands are not excited by a single laser. As regards the proper identification of the LIF peaks we believe that some of them may originate from the dense protein component (conchins) (0.1—5%) as we have used an organic solvent to separate the organic part. We emphasize here that the diffuse band system in the orange sector reported by Konwar et. Al. [11] in a molluscan shell sample in its natural form is due to the orange band system of CaO which is supported by the fact that this band system is excited in carbon arc when $CaCo_3$ is placed in the gap [18]. In Table:1 the most intense line at 734 nm is probably of diatomic origin, preferably the CaO radical in the extreme red system with transition $A^{/}\sum \rightarrow X^{/}\sum$ [18]. Similarly we identify the peak at 720 and 718 nm as persistent line originating from CaO [18]. The medium strong band at 820 and 840 nm are also due to the diatomic radical CaO.

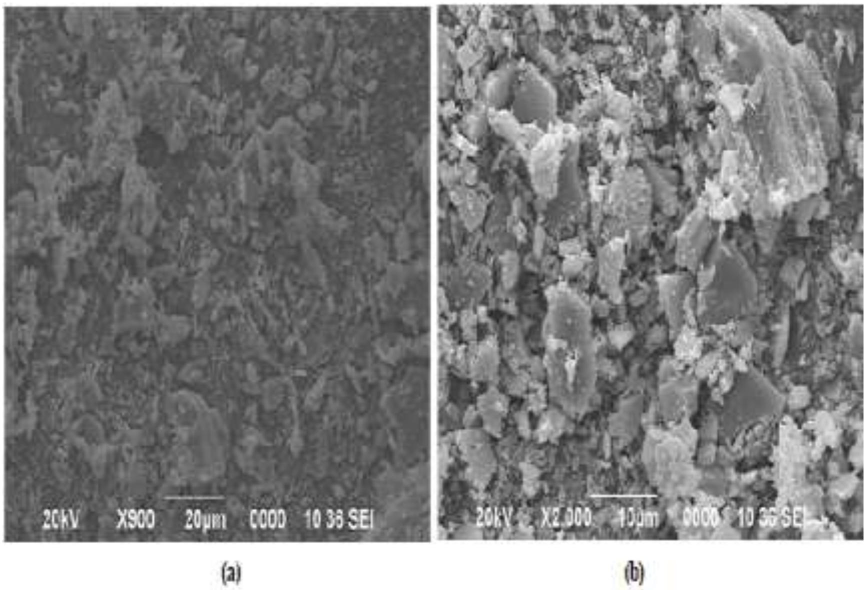

(a) (b)

Scanning Electron Microscopic (SEM) image patterns:

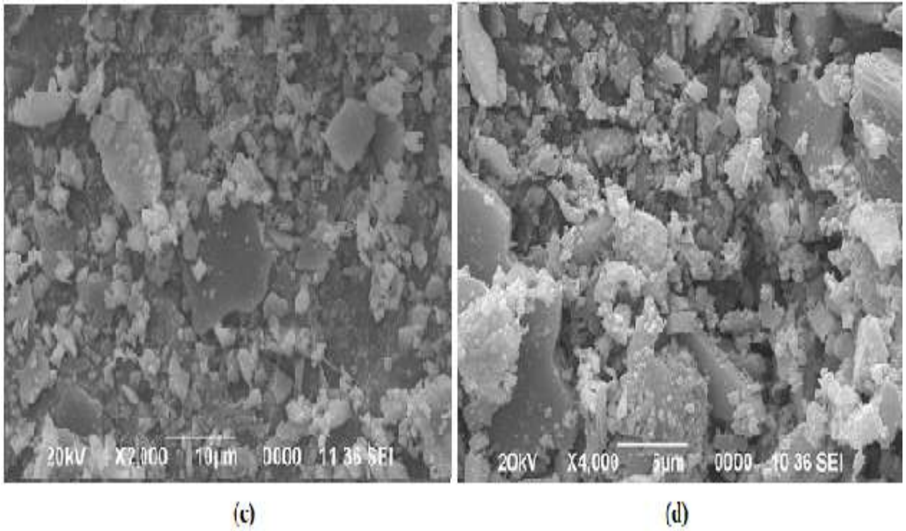

(c) (d)

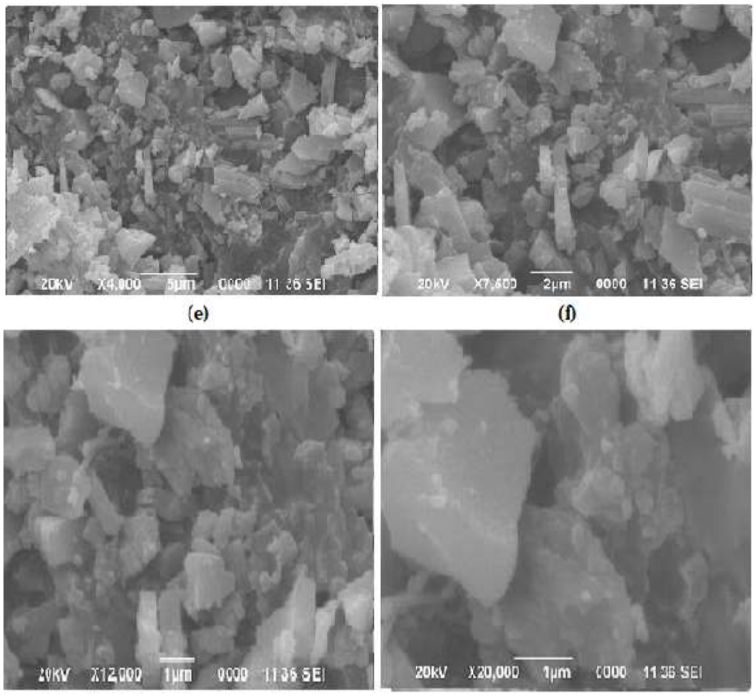

(e) (f)

(g) (h)

Fig: 5 (a, b,........ h) SEM patterns of the powdered specimen of molluscan shell at different magnification

In this section we describe the SEM results obtained from a grinded powered sample of a molluscan specimen. The objective of this work is not to work out a crystallographic texture of the nacreous layer. This is primarily aimed at observing and estimating the size of the grinded material particles along with finding a possible correlation with the iridescent pattern. Fig: 5(a ,b, c, d,……h) show the SEM patterns of the powered specimen of molluscan sample at different magnifications. It will be seen from the SEM patterns exhibited in Fig: 5 that the characteristic feature of the material particles in a molluscan bivalve shell are visualized at successive stages of magnification. It is worthy of remarks here that the SEM images of the grinded powered sample in the present work are highly varied in shapes and sizes. This is expected as we have already mutilated the mollusk shell, by grinding it. Even then one can clearly observe the regular brick wall-like structure which are generally arranged in continuous parallel laminae around 0.5 µm thick (Fig:5 d) separated by sheets of inter lamellar organic matrix [19- 21]. The salient feature of the SEM image at highest magnification (X20,000) (Fig: 5h) shows undoubtedly the existence of numerous microstructures (~0.01µm).

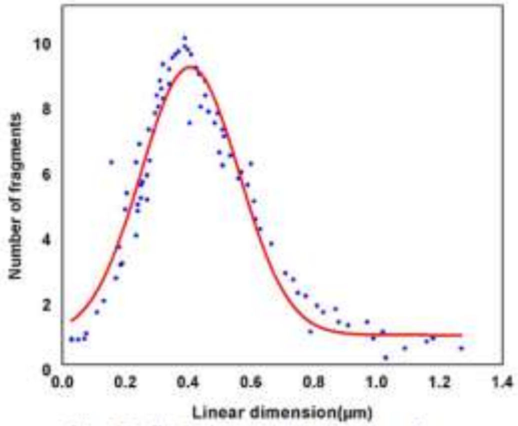

Fig: 6 The distribution pattern of the number of fragments against their linear dimensions

At this stage we find it worthwhile to work out the out the distribution pattern of sizes of various grinded particles which appear in a particular SEM pattern (Fig: 5 c for example) against their number. For this purpose about hundred fragments of different linear dimensions (in µm) against their number have been selected. The distribution pattern is exhibited in Fig:6. The pattern is on a sufficiently small scale to be suitable for exact measurements being made on it with a millimeter scale. Nevertheless a Gaussian pattern emerges as may be inferred from the Fig: 6. the graph is asymmetric in nature. The result is not unexpected. Such types of graphs may be generated in numerous other cases. One may naturally ask, what are the applications of such graphs? One may reasonably believe that they are helpful in characterizing the particular shell.

Summary and Conclusions:-

From what have been described in the earlier sections we sum up the results and draw appropriate conclusions. The foregoing studies are primarily concerned with the iridescence of molluscan shells, laser induced fluorescence of a molluscan shell and scanning electron microscope (SEM) image patterns of a powered specimen. The SEM patterns indicate the presence of numerous gaps between the micro particles and nano structures. A significant fact of observation in iridescence is the patterns of fluctuating luminosity seen and recorded in the Image J intensity distribution patterns. Earlier Raman [9] was of the opinion that the iridescence of mother-of-pearl was a partly diffraction effect that would occur not only when light is incident externally at the surface, but also when it emerges at the surface after suffering reflection at the internal laminations. The optical effects are due to both the surface corrugation and the internal laminations. The present work on the intensity distribution pattern worked out by the software (Image J) and the SEM image patterns presumably supports Raman’s view on iridescence of molluscan shells.

The laser induced fluorescence spectra excited by three different lasers having wavelengths at three different sectors of the spectrum namely blue, green and red, yield interesting results. We infer from Fig: 4 that the spectra consist of two broad and categories. The first category exhibits broad and diffuse bands and the second category exhibits well defined bands. As analyzed in Table: 1, the strong band in the region 460- 600 nm is presumably originates from organic components in the molluscan shell and has not been properly identified yet. Other well defined bands are identified by as belonging to either some persistent lines belonging to CaO or N_2 (1st and 2nd positive). The analysis presented in Table:1 has been made for the first time and it is quite reasonable to believe that it will throw much needed light on the material science associated with the formation of molluscan shells. The distribution pattern of the fragments of the grinded specimen as exhibited in Fig: 6 may also be used to understand the buildup process in a molluscan specimen.

Acknowledgement:-

The author (Konwar. R) is grateful to UGC for award of a minor research project (MRP). No: F.5-390/2014-15/(MRP/NERO) dated 24-03-2015.

The SEM images are recorded at the Department of Physics of Tezpur University.

References:-

1. O B Boggild, Kong. Dsk. Vidensk. Selsk. Skr, Nature. Math. Afd. 2, 230-326 (1930).
2. J D Taylor, W J Kennedy and A Hall Bull, Br. Mus. Natt. Hist. Zool. 3, 1-125 (1969).
3. I Kobayashi, Am. Zool. 9, 663-672 (1969).
4. I Kobayashi, Various patterns of Biomineralization and its phylogenetic significance in bivalve mollusks. In Omori M. Watabe N (eds). The mechanism of Biomineralization in Animals and plants, Tokyo University Press, Tokyo pp 145-155, (1980).
5. C V Raman, Proc. Ind. Acad. Sci. **A**1, 567 (1934).
6. C V Raman, Proc. Ind. Acad. Sci. **A**1, 574 (1934).
7. C V Raman, Proc. Ind. Acad. Sci. **A**1, 859 (1934).
8. C V Raman and D Krishnamurti, Proc. Ind. Acad. Sci. **39**, 1 (1954).
9. G Venkataraman, “Journey into Light”, Life and Science of Sir C V Raman, Penguin Book India (P) Ltd. (1944) p 479.
10. R. Konwar, “Optical and Spectroscopic Studies of some Stratified Media”, Ph. D Thesis, Department of Physics, Dibrugarh University, (India) (2008).
11. R. Konwar, R Changmai and G D Baruah, Indian Journal of Pure & Appl. Phys 42,812-815 (2004).

12. P. H Hare and P.H Abelson; Amino acids composition of some calcite proteins, Carnegie Institution, Washington Year Book, 64, 223-232 (1965).
13. L.P.M Timmermams, Netherlands, Journal of Zoology, 19, 417-523 (1969).
14. Lord Rayleigh, Proc. Roy. Soc. London A103, 233 (1923).
15. L. A. Ramdas, Proc. Indian Assoc. Cultiv. Science 8, 231 (1924)
16. R. Boruah, “Studies on plasmonic and photonic properties of metallic nano structures and their applications”, Ph.D thesis, Tezpur University (India) (2015).
17. W. J. Mitsch, J. G. Gosselink, Wetland, 4th ed. Wiley, New York, NY. USA 2007 [Google Scholar].
18. R. W. B Pearse and A. G. Gaydon, The Identification of molecular spectra, Chapman and Hall Ltd. (London) 1963, p 332.
19. C. Gregoire, J. Biophys. Biochem. Cytol 3, 797-808 (1957).
20. N. Watabe, J. Ultrastruct . Res, 12, 351-370 (1956).
21. S. W. Wise, Eclogae Geol. Helv. 63, 775-797.

Journal Homepage: -www.journalijar.com

INTERNATIONAL JOURNAL OF ADVANCED RESEARCH (IJAR)

Article DOI:10.21474/IJAR01/11530
DOI URL: http://dx.doi.org/10.21474/IJAR01/11530

ISSN NO. 2320-5407

RESEARCH ARTICLE

ON THE NATURE OF THE FLAME EMISSION SPECTRUM OF CRUDE OIL BLAZE AT BAGHJAN

R. Konwar[1], R. Mahanta[2], J. Saikia[3], S. Konwar[4], M. Konwar[5] and G.D Baruah[6]

1. Department of Physics, Tinsukia College, Tinsukia-786125(India).
2. Department of Physics, Dibru College, Dibrugarh-786001(India).
3. Department of Physics, J B College, Jorhat- 785001(India).
4. Department of Petroleum Technology, Dibrugarh University,Dibrugarh-786004(India).
5. Principal, Moran College, Moran- 785670(India).
6. Centre for Laser & Optical Science, New Uchamati, DoomDooma- 786151.

……

Manuscript Info

Manuscript History
Received: 17 June 2020
Final Accepted: 19 July 2020
Published: August 2020

Key words:-
Baghjan Blaze, Spectra, Whispering Gallery

Abstract

A large of flame occurred at Baghjan (27.58309^0 N,95.4018^0 E) as a result of oil well blow out. The present work reports the spectra of the blaze which have been recorded with the help of a Mini USB Spectrometer with spectral range of 200 – 1200 nm. Assignments of the prominent emission and absorption peaks have been made. Apart from the absorption bands of water vapour and atmospheric oxygen the presence of sodium emission line has been identified. On the basis of the assumption that Baghjan flame qualifies as a black body the surface temperature of the flame has been estimated to be approximately 4140^0 K. Whispering gallery made in atmosphere has been proposed to explain the roaring sound that can be heard from a distance of 15 Km from the blaze.

……

Introduction:-

Flames are sources of many band system of diatomic and polyatomic origin. Some bands are observed by the direct combustion of inflammable substances, others by the introduction of additional substances into a flame already established. Flame bands have been found to belong to molecules which are electrically neutral, but very frequently the molecules are not stable in a chemical sense thus combinations such as CH, NH, CN and OH are very common occurrence [1,2]. The general characteristics of the band systems obtained in this way arise from transitions between a few of the lowest levels of the molecules concerned. The energy of the upper levels involved nearly exceeds 5 eV while the lower level is in most cases the ground state. The 4300 Å and 3900 Å band of OH and Swan band of C_2 appear readily enough in the flames of hydrocarbons. Different systems occur most strongly in different parts of the flame. The OH bands are spread through the blue outer cone of a Bunsen flame using coal gas, but the Swan bands are restricted to the greenish inner core of the roaring flame which owes its colour mainly to the presence of these bands. The red and violet systems of CN are given by a flame of moist cyanogens. The 3360 Å band of NH is also obtained strongly from the oxy-ammonia flame, but the systems arising from more excited levels, which are known from other sources, do not appear as well.

From the descriptions as given above it would follow that flames are well known sources of many diatomic radicals. The aim of the present work is to describe the nature of the spectrum in the visible sector originating from a huge flame of fire that engulfed Well No 5 at Baghjan oil field (27.58309^0 N, 95.4018^0 E). Such gas and crude oil blow

Corresponding Author:- R. Konwar
Address:- Department of Physics, Tinsukia College, Tinsukia-786125(India).

out is believed to be rare event and its second of its kind in recent years in India, the earlier one took place in the year 2005 at Dikom (94.6^0 E , 27.3^0 N) [3] which is about 50 Km away from Baghjan. In the present work we will have occasion to make a comparative study of the spectra of the blazes which occurred at different places and at different times.

Experimental:

Origin of the blaze: On June 9, 2020 an oil well under Oil India Limited at Baghjan (27.58309^0 N, 95.4018^0 E) located close to the Maguri Beel (wet land) a huge flame of fire occurred as a result of sudden and accidental outburst. The blaze at the well is so massive that it can be seen from a distance of 30 Km with the flame with black smoke going up about 100 meters high endangering local biodiversities in the Dibru- Saikhowa National Park which is adjacent to Baghjan. The spectra of the blaze have been recorded with the help of a Mini USB Spectrometer with spectral range of 200 – 1200 nm. The nearest distance from the blaze to the spectrometer is about 120 meter. Light from the blaze is allowed to fall on the objective of a small telescope and is collected at the eyepiece. The opening end of the optical fiber is kept in close proximity of the eyepiece and the other end of the optical fiber is connected to the spectrometer. A lap-top where an appropriate software is installed to record the spectrum is connected to the spectrometer (Mini USB Spectrometer, Model: SP2 (V 2.1) (LISUN GROUP http:www.lisungroup.com). Fig: 1 shows the spectrum of the blaze recorded on the spectrometer. It is worthy of remark that the experiment is carried out at night and at 20 Hrs. to avoid any extra radiation from the sun which is present during day time. For consideration of comparison a solar spectrum has also been recorded on the same spectrometer. This is exhibited in Fig: 2.

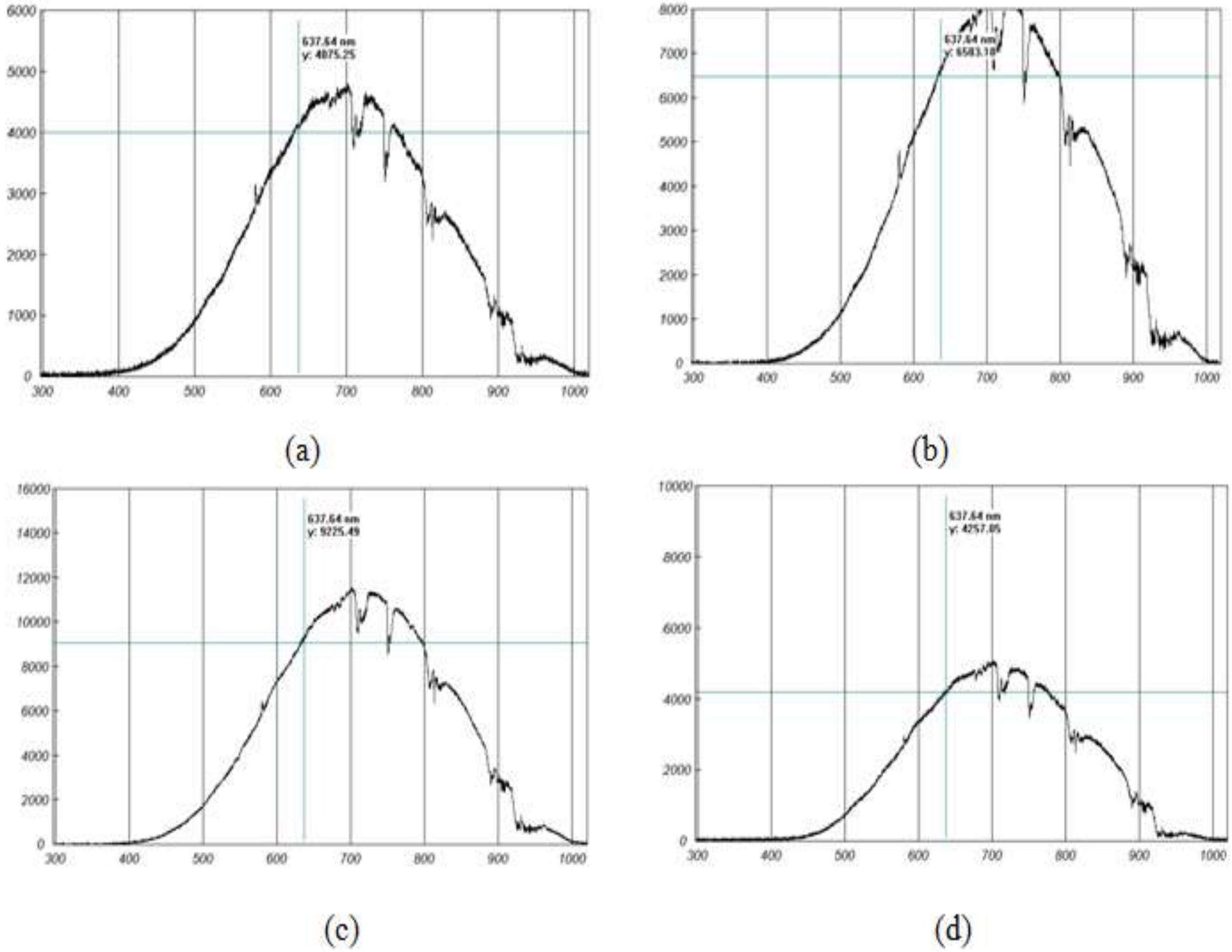

Fig: 1(a, b, c, d): Spectrum of the Baghjan blaze recorded on a Mini Spectrometer (Model SP2 V2.1) on June 16, 2020

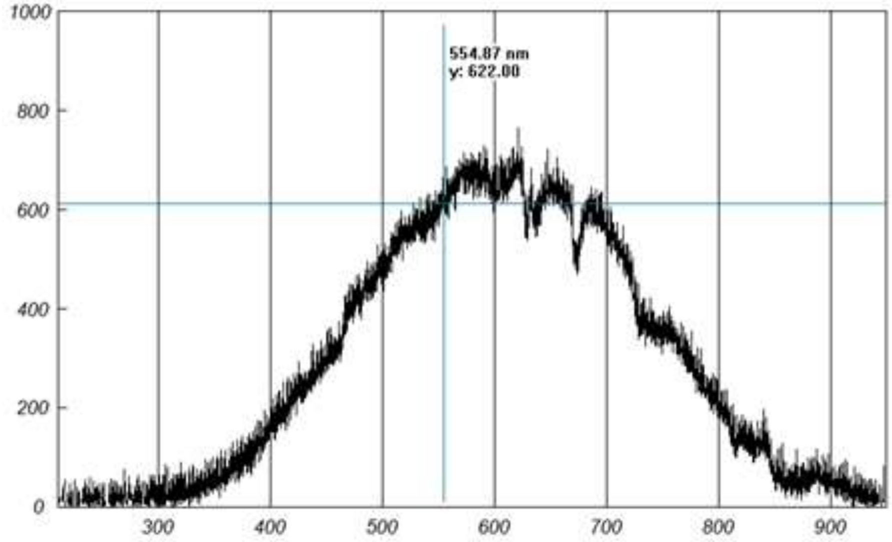

Fig. 2:- Spectrum of the sun recorded on the Mini spectrometer (Model SP2 V 2.1).

Results and Discussion:-

Let us first try to estimate the surface temperature of the flame from a consideration set forth above. From Fig 2 we have an estimate of the surface temperature of the sun as follows. The sun emits radiation over a wide range of wavelengths. We assume that sun is a black body. In this case the radiation is given by the Planck’s equation

$$I(\lambda)\Delta\lambda = \frac{2\pi hc^2}{\lambda^5}\frac{1}{e^{hc/\lambda kT}-1}\Delta\lambda$$

where $I(\lambda)\Delta\lambda$ is the emitted energy per unit area of black body per unit time within the range of wavelength $\Delta\lambda$, measured at absolute temperature T and k is Boltzmann’s constant.

Graphs for several temperatures can be drawn. From these curves one can see that the peak wavelength is given by Wien’s displacement law

$$\lambda_{\max} = \frac{2.898\times10^{-3}mK}{T}$$

Taking 5778^0 K as the surface temperature of the sun the peak wavelength is about 501 nm. This is the blue green part of the visible spectrum, or the range of frequencies that our eyes can see. It is worthwhile to note that solar spectrum as shown in Fig:2 shows few well known Fraunhofer intense absorption lines at 6276 – 6278 Å known as α line due to atmospheric O_2, at 6867 – 6884 Å known as B line due to atmospheric O_2 and at 7594 – 7621 Å, the A line due to atmospheric Oxygen. As may be inferred Fig: 1 the spectrum of Baghjan flame shows the peak wavelength at 700 nm which is shifted towards red considerably as compared to the solar spectrum. However, on the basis of the assumption that the Baghjan flame qualifies as a black body the peak wavelength is given by the equation as given above and we have as a surface temperature of the flame

$$T = \frac{2.898\times10^{-3}mK}{700} = 4140^0 K$$

There are additional characteristics which may be seen in the emission profile of the Baghjan flame. The emission line of sodium appears at 5893 Å. This is however, is weak as compared to the emission line of sodium which is the most intense line in the emission profile of Dikom fire [3, 4]. The presence of a very intense line of Na in the crude oil blaze at Dikom and also in the Baghjan blaze where the Na line appears rather weakly indicates some geophysical characteristics of the region far below the surface. In addition to the Na lines there are other spectral characteristics which may be observed in the spectrum of the Baghjan flame. The atmosphere around the blaze is surrounded by an envelope of hot gases which are product of the combustion processes. The emission from the from the blaze has to pass through this blanket of gases and vapours before it is recorded by the spectrometer. This results in absorption features in the spectral profile. It is possible to make assignment to the absorption bands and as well as to the emission peaks. It may be added that the CN red system of bands which was present in the spectrum of Dikom fire is not observed in the spectrum of Baghjan flame. Table: 1 has been prepared to exhibit the prominent lines and appearing in the Baghjan spectral profile.

Table 1:- Spectral profiles of Baghjan flame and assignment of the prominent emission and absorption peaks.

Wavelength (nm)	**Intensity**	**Emission**	**Absorption**	**Assignment**
589	w	emission	--	Sodium (Na) D line
676	ms	emission	--	N_2 1st positive
682	ms	emission	--	CO
688	ms	emission	--	O_2, atmosphere
694	ms	emission	--	H_2O
709	s	--	absorption	H_2O
718	s	--	absorption	H_2O
753	s	--	absorption	O_2, atmosphere
806	s	--	absorption	H_2O
815	s	--	absorption	H_2O
827	s	--	absorption	H_2O
899	ms	--	absorption	H_2O
900	ms	--	absorption	H_2O
938	ms	--	absorption	H_2O
950	ms	emission	--	H_2O

w = weak, ms = medium strong, s = strong

As may be inferred from Table:1, most of the spectral features have been identified as belonging to H_2O and atmospheric O_2 molecules. In assigning the bands we taken help from the classic books of Pearse and Gaydon [1, 2] and other references [5, 6, 7]. It is well recognized that atmospheric and infrared absorption (vibration – rotation spectrum) by H_2O molecules in vapour appears especially in solar spectrum. The bands are complex and shows fairly open rotational structure, but no obvious heads. Visible and infrared emission is a part of the vibration – rotation spectrum of H_2O. The infrared and red bands appear readily in flames but the visible bands are very weak and are given by a flame of oxygen burning in hydrogen. The system is complex and in the visible the maximum of intensity are due to bunching of lines of complex rotational structure and the heads are not very definite; to the longer wavelengths, however, some of the bands show sharp heads and are degraded to the longer wavelengths. It is worthy of remark that liquid water shows infrared absorption bands at about 7750Å and 9850 Å. All these characteristic features are present in the spectrum of Baghjan blaze. We may note here that the CN – red system which was present in Dikom flame [3,4] is conspicuous by its absence in Baghjan flame. We may appropriately conclude this section with a comment that Baghjan flame spectrum is quite analogous to the Fraunhofer spectrum or the solar spectrum with a difference that the peak wavelength in Baghjan spectrum is shifted to the red as compared to the solar spectrum. We have also considered the Baghjan flame as a black body.

Whispering gallery mode:

In this section we discuss the whispering gallery mode associated with the Baghjan blaze. This is for the first that whispering gallery mode has been linked with any flame. It is worthwhile to note that the roaring sound of Baghjan blaze can be clearly heard from a distance of fifteen kilometers from the source. It is also observed that this particular sound is not audible to an observer who is in close proximity of the blaze (say about 500 meters from the blaze). This is curious but the phenomenon may be explained if we take into account the whispering gallery mode to operate in the atmosphere. We note here that in a cloudy weather the sound of the Baghjan blaze is more prominent than in a clear weather. It naturally prompts us to identify that the atmosphere is the key factor.

Whispering gallery waves or whispering gallery modes are a type of waves that can travel around a concave surface. A whispering gattery is usually a circular, hemispherical, elliptical or ellipsoidical enclosure often beneath a dome or vault in which whispers can be heard clearly and loudly in other parts of the gallery. Such galleries can also be set up using two parabdolic dishes. Sometimes the phenomenon is also detected in caves. In fact there are numerous instances that exhibit such modes. Lord Rayleigh developed the wave theories for the whispering gallery in St.

Paul's Cathedral London in 1910 and 1914[8]. Fitting sound waves inside a cavity involves the physics of resonance based on wave interference. Sound can exist only at certain pitches as in the case of organ pipes. Whispering gallery waves are guided by the effect of the wave curvature. Raman and Sutherland [9] performed an extensive series of experiment and observed multiple bands. Rayleigh's theory predicted only one band, whereas Raman's experiment revealed the existence of many Rayleigh's theory obviously needed an extension which Raman did not attempt. The acoustics of Baghjan blaze gives us an opportunity to investigate it from the point of view of whispering gallery mode.

Conclusions:-

We now sum up the results which have emerged in this work and also draw appropriate conclusions. The huge blaze of Baghjan flame which occurred as a result of blow-out of a oil well at Baghjan in upper Assam has caused damage to the environment and loss of human life including loss of rig and equipments. We have recorded the spectra of the flame with the help of a mini spectrometer and with the help of the spectrum the surface temperature of the flame has been estimated to be 4140^0 K. Apart from the absorption bands of water vapour and atmospheric oxygen the presence of sodium emission indicates some geophysical characteristics of the region lying deep inside the surface. A comparison of Dikom blaze, a similar event that occurred at Dikom about fifteen year back, showed spectral characteristics which are different from those of Baghjan flame. But the emission line of Na is extremely strong in Dikom flame. An unexplained sound with occasional tremor associated with Baghjan oil well fire that can be heard even from a distance of fifteen kilometers can be linked with atmospheric whispering gallery mode. We may appropriately conclude this section with a remark that though nature has given us an opportunity to make scientific investigation of hazardous oil well blaze at Dikom and Baghjan, we should be equally concerned with the loss of human life and with the damage to the environment.

Acknowledgement:-

Authors are thankful to the security personals who allowed the spectra to be recorded at a place in the vicinity of the blaze. They are also thankful to S Bhowmic who helped in the experiment.

References:-

1. R.W.B. Pearse and A.G. Gaydon, Identification of Molecular Spectra, Chapman and Hill Ltd., London (1963).
2. A.G. Gaydon, Spectroscopy of Flames, Chapman and Hill Ltd., (1957).
3. M. Konwar, N Dehingia and G.D. Baruah, Advances in Applied Science Research, 2(4), 98-101 (2011)
4. N. Dehingia, M. Konwar, N.C. Sarmah and G.D. Baruah, Contemporary Optics and Optoelectronics, Ed. PP Sahu, P Deb, Tata McGraw-Hill Publishing Co. Ltd. (2007) pp 247-248.
5. W. Baumann and R. Mecke, Z. Physik 81, 445(1933)
6. K. Freudenberg and R. Mecke, Z Physik , 81, 465(1933)
7. A.G. Gaydon, Proc. Roy. Soc. 181, 197(1942).
8. Lord Rayleigh, Scientific Papers, (Cambridge University Press, Cambridge, 1912) Vol V, p 617.
9. C. V. Raman and G.A. Sutherland, Proc. Roy. Soc. London, A 100, 424 (1921).

On The Nature Of Iridescent Patterns Of Some Molluscan Shells

Konwar R, BARUAH. G. D

Department of physics, Tinsukia College, Tinsukia-786125, India.
Centre for Laser and Optical Science, New Uchamati; Doom Dooma-786151, India
E-mail: konwar_rajib@rediffmail.com

Abstract: The present work is concerned with the iridescent patterns of some specimens of molluscan shells and their intensity distribution patterns worked out with the help of software. The iridescence colours of shells have been ascribed to diffraction and their laminated structures. In this case earlier observations by Sir C. V. Raman in connection with the iridescent patterns have been critically analysed.

Keywords: Iridescent patterns, Molluscan shells.

1. Introduction:

Molluscan shells have attracted the attention of researchers for many interesting physical phenomena exhibited by these objects. The materials of the molluscan shells present different appearances in different cases. The shell of a molluscan built out of calcium carbonate has 3000 times higher fracture resistance than crystals of calcium carbonate. Several decades ago Raman and his coworkers[1-5] investigated experimentally various optical properties including iridescent patterns. Recently Konwar[6] and Konwar et. al[7] have investigated the laser induced fluorescence and other spectroscopic properties of few molluscan shells. It is worthwhile to note here that in spite of the extensive work done during several decades on various aspects of molluscan shells, the emergence of the field of nanoscience has greatly influenced the field of bio-mineralization. In the present work we primarily concerned with the iridescence colours of some Molluscan shells, and their analysis with the help of software known as Image J which is primarily used for the measurement of intensity.

2. Iridescence colours:- What they are?

The iridescence patterns of the molluscan shell are the coloured patterns which are usually seen under normal condition of illumination in some molluscan shells. The iridescence colours of shells have been ascribed to either interference or diffraction, while the diffraction component is well established to account for the multicoloured iridescent colour component in shells; the origin of changes in body colour in the case of pearl has not been clearly established. Lord Rayleigh[8] was also interested in iridescent colour and the physics behind the process of iridescence, and one of his papers is devoted to iridescent beetles. Similarly as early as in 1923 Ramdas[9] had investigated feeble iridescence from potassium chlorate crystal. Potassium chlorate belongs to the monoclinic class of crystal, and its natural occurrence takes the form of flat plates containing many twins, when a crystal plate is held so as to reflect light obliquely and is turned around in its own plane, colours alternately appear and disappear twice in each complete revolution. The spectral character of the reflected light also varies with the angle of incidence. In a recent work[10] the author has described how butterfly wings involve nano system particularly the photonic band.

3. Iridescent patterns of Molluscan shells and 3D intensity distribution patterns:

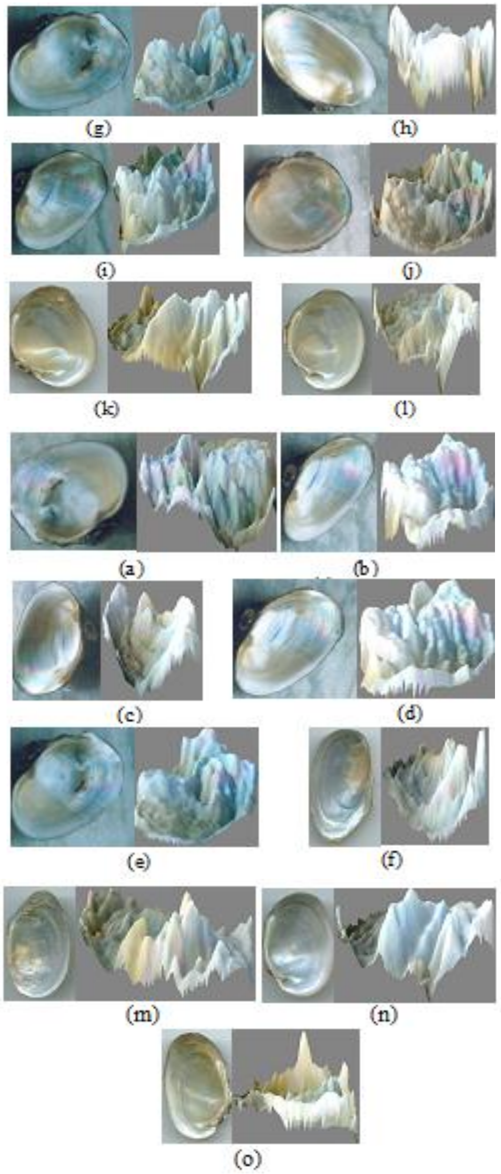

Fig:1 Iridescence pattern of molluscan shells and their three dimensional intensity distribution patterns.

Fig:1(a,b,c,… ……,o) shows the surfaces of molluscan shells under illumination by a broad band light of a scanner connected to a computer. We have used software (Image-J) to work out the three dimensional intensity distribution patterns of the iridescent molluscan shells. It may be noted that the colours exhibited by these photographs are actually the manifestations of the optical properties associated with the relative thickness of the conchin and aragonite layers in different specimens of shells. A close examination of the intensity distribution pattern show several sharp peaks on the background and these are actually conchin layers intersected with the surface of the shell and their configuration depends upon the curvature of the intersecting surfaces and the angle at which they meet. We thus find that the method of three-dimensional intensity patterns gives qualitative information about the nature of iridescent patterns. In this connection we would like to indicate the nature of the laser induced fluorescence (LIF) of some specimens of molluscan shells which have been earlier investigated by us[6]. The salient features of the LIF spectra are shown in Table:1.

***Table: 1** Laser induced fluorescence band systems of ten different samples of Molluscan Shells.*

Sample no.	Range of wavelength (Å)	Intensity	Wavelengths of the persistent pair	Intensity	Iridescence observed
a	5900-6650	s	5372.8, 5407.1	w	YES
b	5850-6600	s	5372.8, 5407.1	w	YES
c	5800-6300	vs	5372.8, 5407.1	vs	YES
d	~	vw	5372.8, 5407.1	vs	YES
e	5800-6700	s	5372.8, 5407.1	w	NO
f	5850-6700	vs	5372.8, 5407.1	s	YES
g	5850-6700	vs	5372.8, 5407.1	vw	NO
h	5800-6900	vvs	5372.8, 5407.1	vvs	YES
i	5800-6900	vvs	5372.8, 5407.1	vw	NO
j	~	vw	5372.8, 5407.1	w	NO

vvs = very very strong, vs = very strong, w = weak and vw = very weak.

We have noted earlier in the case of LIF of molluscan shells, that the molluscan shells exhibit strong fluorescence in the yellow – red region with a pair of weak band heads also appearing with moderate intensity. They have been identified with the persistent lines belonging to the First Positive band system of N_2 molecule. It is worthwhile to note as shown in Table:1, iridescent patterns do not appear in case of shells which do not exhibit fluorescence or exhibit fluorescence with extremely weak intensity.

4. Conclusion:

From what has been discussed above it is appropriate to make a conclusion regarding the iridescent patterns of molluscan shells. The iridescent patterns of the shells depend on their laminated structures.

Acknowledgement:

The author (Konwar. R) is grateful to UGC for award of a minor research project(MRP). No: F.5-390/2014-15/(MRP/NERO) dated 24-03-2015.

References:

[1] C V Raman, Proc. Ind. Acad. Sci. **A1**, 859(1934).

[2] C V Raman, Proc. Ind. Acad. Sci. **A1**, 567(1934).

[3] C V Raman, Proc. Ind. Acad. Sci. **A1**, 574(1934).

[4] C V Raman and D Krishnamurti, Proc. Ind. Acad. Sci. **39**,1, (1954).

[5] G. Venkataraman, “Journey into light” Life and Science of Sir C V Raman, Penguin Book India (P) Ltd. (1994) p479.

[6] R. Konwar, “Optical and Spectroscopic Studies of Some Stratified Media” Ph.D Thesis in Physics, Dibrugarh University, India (2008).

[7] R. Konwar, R. Changmai and G. D. Baruah, Indian J. Pure & Appl. Phys. **42**, 812-815(2004).

[8] Lord Rayleigh, Proc Roy. Soc. London A103,233(1923).

[9] L. A. Ramdas, Proc. Indian. Assoc. Cultiv. Science, **8**, 231(1924).

[10] R. Boruah, “Studies on Plasmonic and photonic properties of metallic Nanostructures and their applications” Ph.D Thesis, Tezpur University,(India) (2015)

ISSN NO. 2320-5407

Journal homepage: http://www.journalijar.com
Journal DOI: 10.21474/IJAR01

INTERNATIONAL JOURNAL OF ADVANCED RESEARCH

RESEARCH ARTICLE

Vector Representation and Fibonacci Numbers in Molluscan Shells.

***R. Konwar[1] and G.D.Baruah[2].**

1. Department of Physics, Tinsukia College, Tinsukia-786125.
2. Centre for Laser & Optical Science, New Uchamati, DoomDooma-786151.

Manuscript Info

Manuscript History:

Received: 17 February 2016
Final Accepted: 12 March 2016
Published Online: April 2016

Key words:
Molluscan shells, Fibonacci numbers,Vector representation.

****Corresponding Author***

Enas Mohamed Attia.

Abstract

The present work describes the growth of a particular species of Molluscan shell in terms of moving vectors. The appearance of Fibonacci numbers in Molluscan shell has been identified.

Introduction:-

Molluscan shells have attracted the interest of research workers for many physical phenomena exhibited by the materials. The shells is created by a living pulsating creature around itself as a cover for defence and it represents some type of permanent phase which is irreversible. The materials of the molluscan shells present different appearances in different cases. The shell of a molluscan built out of calcium carbonate has 3000 times higher fracture resistance than crystals of calcium carbonate. Shell growth involves increase in both area and thickness. Increase in area is a function of increase of mantle and increase in thickness relates to the deposition of calcium carbonate and organic matrix. The reference points for all analysis of "bivalve" shell grows are the "unibones"; the oldest part of the shell. The majority of bivalves contain chromo-proteins associated with the conchiolin of their shell valves and many of the melaninoid pigments may owe their origin to the biochemical activities associated with the quinone tanning of conchiolin. Several decades ago Raman and coworkers[1-5] investigated experimentally various optical properties like iridescence and optical characters of shells. According to Raman [5] the external form of the shell and the internal architecture of its substance are intimately related to each other. While one may not know yet whether the beautiful patterns on the shell surface have a functional role, one is at present time at least able to explain how such patterns could arise. As in the case of Liesegang precipitation[6,7], it appears that certain non-linearities called into play during the shell growthare the controlling factors. Meinhart and Klingler[8] have succeeded simulating many of the observed shell patterns using a suitable non-linear reaction diffusion model. In bio-mineralization field, the mollusk shell is one of the best studied of all calcium carbonate bio-minerals. Particular attention has been given to organic matrix [9-13]. The organic matrixwhich promotes the nucleation of the mineral component to direct the crystal growth and is supposed to act as glue to prevent the fracture of the shell has been given particular attention [14-17]. The main biopolymers present in the organic matrix are essentially proteins, either glycosylated or acidic polysaccharides and chitin. In nacre they represent 1-5% (w/w)of the structure. The nacreous layer of Molluscan shell has been studied extensively for several decades particularly with X-ray and electron microscopic techniques. This work has been largely successful in describing microstructure of nacre [18-22]. Various calcium binding, highly acidic, water soluble proteins have been isolated from the shell in the various stages of development [23]. The process of purification and characterization of calcium binding conchiolin shell peptides from the Molluscan has been investigated by Cariolou and Morse [23] and also by others. Water soluble proteins from the shell have been characterized by X-ray diffraction leading to the conclusion that they resemble fibroin [24].

Both the water soluble and water insoluble proteins have been proposed as multilaminar templates for the mineral tablets [25]. The mechanism of growth of nacreous layer is complex and is not completely understood in spite of investigation of several decades. It is known that both organic and inorganic components are secreted by epithelial cells in the mantle tissue into the extrapallial space (the extra cellular cavity between the mantle and the shell which is sealed from the surrounding environment), bathing the growing shell in a mixture called the extrapallial fluid. It was Kitano and Hood [26] who first showed that aragonite is the most favorable phase of calcium carbonate ($CaCO_3$) to nucleate in sea water supersaturated with respect to that mineral. The submicroscopic structure of the conchiolin of the prisms in Molluscan shells has been extensively studied several decades ago by Gregoire [27,28]. It was established that the inorganic part of a prism is made up of calcite crystals piled one upon the other, the pile being wrapped into a conchiolin sheath built upon a fabrillar structure covered by a very dense protein component. The active role of proteins in biomineralization is a fundamental issue and has been described by several workers [29, 30]. It represents a source of inspiration for nanotechnology. The brick and mortar ordering of nacre (mother of pearl) has already inspired the toughening of ceramics materials by co processing rigid ceramics as silicon carbide and compliant interlayer as boron nitride [31]. The interdigitating brickwork array of tablets of sheet nacre is not only the only interesting aspects of nacre structure. The bio crystal itself is a composite. The spatial organization of the bio mineralization mechanism of the crystal growth is the main focus of the recent years [32]. Laser induced fluorescence spectra of few species of Molluscan shells were also recorded by Konwar et. Al. [33] and the salient features of the spectra were a strong diffuse band in the red yellow sector along with the persistent pair of band heads at 5407.1 Å and 5372.8 Å. These pairs of band heads appearing in the spectra are due to the First positive bands of molecular nitrogen.

We have indicated here a brief overview of the works and investigations carried out on Molluscan shells during last several decades. In the present work we shell consider the phenomenon of the evolution of the growth pattern of the shells and their representation in terms of vectors. The regular spacing of the external growth rings on shells and their progressive crowing as the Mollusks grow older continue to prompt researchers to interpret them as age makers, analogous to annual rings in some trees. Despite extensive study, however, the use of external growth patterns in most species has been found to be rather limited. In the present work we specifically discuss, for the first time, the appearance of Fibonacci numbers in Molluscan shells. This seems to be connected with the phenomenon of "Antisymmetry" which is seen as a part of biological evolution of plant and animal species [34].

Evolution of elliptical patterns and Vector representation:-

The Molluscan shells which I have procured from *Maguri bill*, near Dibru Saikhowa National Park, Tinsukia, Assam was used as specimens for our work. Fig. 4.1 (a, b, c, d, e, f) shows the photographs of six specimens of Molluscan shells along with the growth patterns represented as moving vectors. The vectors are drawn by taking the centre of an ellipse as a starting point of a vector and connecting the successive centres of the ellipses. It is worthwhile to note that some sort of oscillatory pattern is maintained as these vectors evolve

in time. In some cases such as Fig 1(e), the oscillatory pattern is more apparent. Anyone who is experimentally familiar with the production of Liesegang rings in gelatin films and other allied phenomena might be tempted to believe that such periodic precipitates are analogous to the periodic growth of the elliptical patterns. In Molluscan shells exhibited in Fig 1 the individual rings are so crowded together that it is not possible to observe them separately. Rings up to a maximum number of thirty only could be observed.

(a)

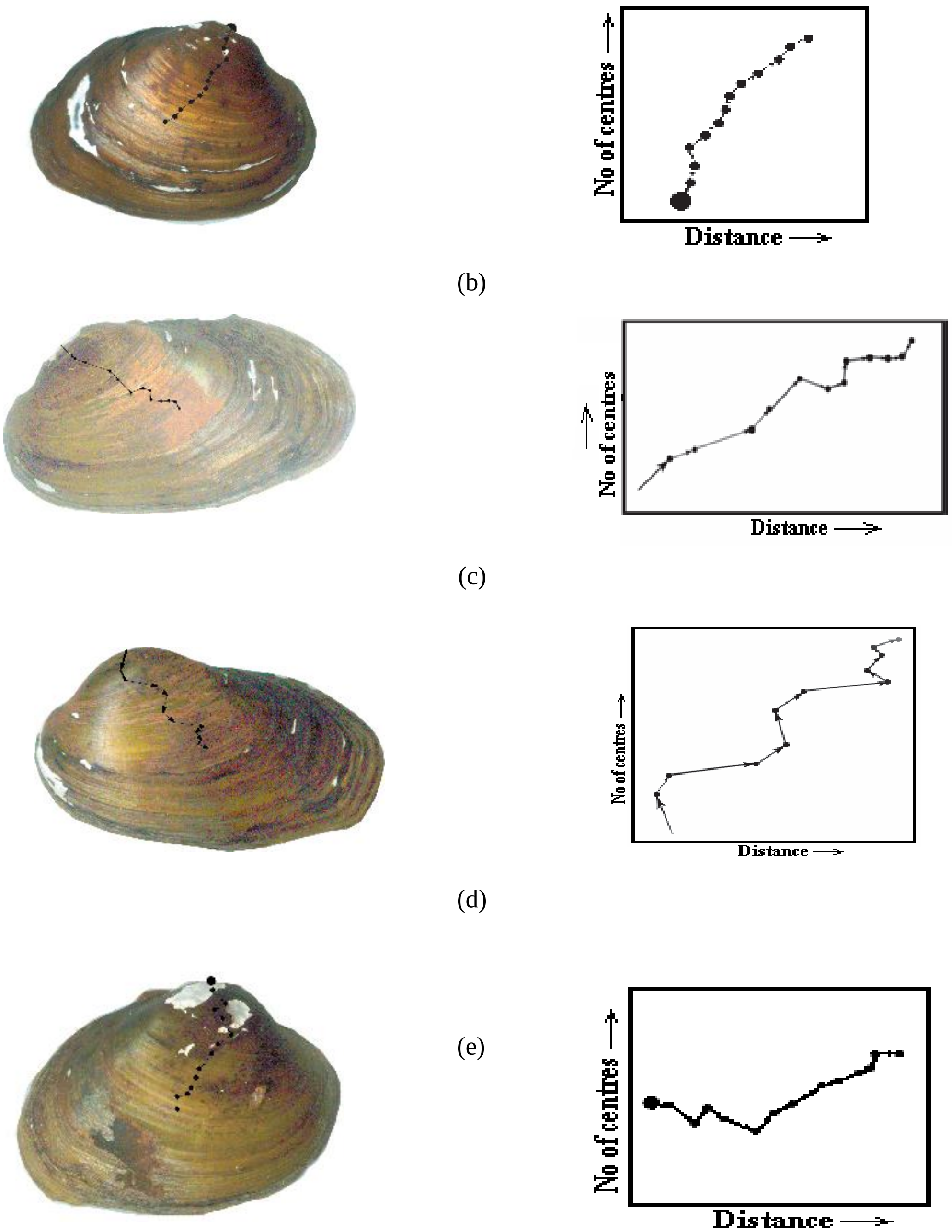

(b)

(c)

(d)

(e)

(e)

Fig 1 (a, b, c, d, e, f) Vector representation of the growth of Molluscan shells

Fibonacci Numbers in Molluscan Shells:-

The Fibonacci numbers are the sequence of numbers $\{F_n\}_{n=1}^{\infty}$ defined by the linear recurrence equation

$$F_n = F_{n-1} + F_{n-2} \quad \dots \dots \dots \dots \dots \dots \quad (1)$$

with $F_1 = F_2 = 1$. As a result of definition (1) it is convenient to define $F_o = 0$. The Fibonacci number for n = 1, 2, 3, ………… are 1, 1, 2, 3, 5, 8, 13, 21, 34, …………….. These numbers seems to appear in the Nature in numerous cases. It is worthwhile to note that the succeeding terms of the system are obtained by the sum of two preceding terms being with the lowest whole number; thus 1, 2, 3, 5, 8, 13, 21, 34, 55, 89, 144 etc. This converging series of numbers is also known as a Fibonacci series, because it was first noted by Leonardo da Pisa, called Fibonacci. Gerard, a mathematician of the 17th century, also drew attention to this strange system of numbers because of its connection with the celebrated problem antiquity, namely, the eleventh proposition of the second book of Euclid. Its relation to the phenomenon of planet growth is brought out by Church[35], who uses a sunflower head to explain the phenomena.

Few other characteristic properties of Fibonacci series are that if we take three consecutive numbers, the square of the middle term and the difference between the multiplication of the first and third terms is always the same. Mathematically we have

$$F_{n-1} \times F_{n+1} - F_n^2 = (-1)^n \quad \dots \dots \dots \dots \dots \quad (2)$$

In Fibonacci series for any four consecutive terms (A, B, C, D), $C^2 - B^2 = A \times D$

For example in case of (2, 3, 5, 8)

$$5^2 - 3^2 = 8 \times 2, \quad 16$$

Mathematically we have

$$F_{n+2}^2 - F_{n-1}^2 = F_n \times F_{n+3} \quad \dots \dots \dots \dots \dots \dots \quad (3)$$

Any term in the series can be expressed by the equation

$$F_n = \frac{r_1^n - r_2^n}{r_1 - r_2} \quad \dots \dots \dots \dots \dots \dots \quad (4)$$

Here r_1 and r_2 is the root of the quadratic equation.

$$x^2 - x - 1 = 0, \quad \text{that is}$$

$$r_1 = \frac{1+\sqrt{5}}{2} \qquad \text{and} \qquad r_2 = \frac{1-\sqrt{5}}{2}$$

The closed form of (4.4) is therefore given by

$$F_n = \frac{\left(1+\sqrt{5}\right)^n - \left(1-\sqrt{5}\right)^n}{2^n \sqrt{5}} \quad \dots \dots \dots \dots \quad (5)$$

Again, leaving aside few small terms, if we take the ratio of two consecutive terms then the ratio always remain the same, and it is equal to 1.618. So the number is known as the divine number.

Fig1 shows the photographs of few specimens of shells. If we take the semi-major axes of the successive prominent elliptical rings we observe that the ratio of the distances (taken arbitrarily in millimeters) of the semi-major axes remains nearly constant and approaches the so called divine number as identical earlier(Table-1)

Table I

Ring No	Semi-major axis (in mm)	Ratio in successive rings	Difference from the divine number, 1.618
1	5	--	
2	8	1.600	+0.018
3	13	1.625	-0.007
4	21	1.615	+0.003

Summary and Conclusion:-

In the present work we introduce the concepts of moving vectors and Fibonacci numbers in naturally occurring Molluscan shells. It is reasonable to believe that the investigation will give additional insights into the secret of evolution of the Molluscan shell.

Acknowledgement:-

The author (Konwar. R) is grateful to UGC for award of a minor research project (MRP). No: F.5-390/2014-15/(MRP/NERO) dated 24-03-2015.

References:-

1. C V Raman, *Proc. Ind. Acad. Sci.* **A1**, 859(1934).
2. C V Raman, *Proc. Ind. Acad. Sci.* **A1**, 567(1934).
3. C V Raman, *Proc. Ind. Acad. Sci.* **A1**, 574(1934).
4. C V Raman and D Krishnamurti, *Proc. Ind. Acad. Sci.* **39**,1, (1954).
5. G. Venkataraman, *"Journey into light"* Life and Science of Sir C V Raman, Penguin Book India (P) Ltd. (1994) p479.
6. K Subba Ramaiah, *Proc. Indian Acad. Sci*. **A9**, 455(1339).
7. K Subba Ramaiah and C V Raman, *Nature (London)* **142**, 355(1938).
8. H. Meinhard and M Klingler, *J. Theo. Bio* **126**, 63(1987).
9. M A Crenshaw, *Biomineralization*, **6**, 6-11(1972).
10. G Kranmpitz, J. Engels and C Cazawx, *"Biochemical studies on water soluble proteins and related components of gastropod shells"* In the mechanisms of Mineralization in the Invertebrates and Plants. (Watabe, N & Wilbur, K M, eds), pp 175-190. The B. W. Barush Libray in Marine Science no. 5, The University of South Carolina Press, Columbia.
11. S. Weiner, W. Traub and H A Lowenstam. *Organic Matrix in calcified exoskeletons. In Biomineralization and Biological Metal accumulation.* (Westbrock, P& DeJong, E.W eds) pp-205-224(1983), Reidel, Wordrecht, Holland.
12. J Keith, D Stockwell, D Ball, K Remillard, D Kaplan, T Thannhauser and R Sherwood, *Comp. Biochem. Physiol*. **105B**, 487(1993).
13. Y Levi-Kalisman, G Falini, L Addali & S Weiner *J. Struc. Biol*. **135,** 8-7(2001).
14. S Weiner and L Hood, *Science* **190**, 987-989(1975).
15. A M Belcher, X H Wu, R. J Christiansen, P K Hansma,G D Stucky and W E Morse. *Nature* **381**, 56-58(1996).
16. S Weiner and W Traub, *Phil. Trans. R Soc. Lond.***B304**, 425-434(1984).
17. S Kamat, X. Su, R Ballarini and A H Heuer, *Nature* **405**, 1036-1040(2000).
18. H A Lowenstam and S Weiner, *On Biomineralization*, Oxford University Press, New York, (1989).
19. S Weiner *CRC Crit Rev. Biochem*, **20,** 356-408(1986).
20. N Watabe. *Prog. Crystal Growth Charact*, **4**, 99-147(1981).
21. K M Towe, *Bull. Natl. Pearl Res. Lab. JPN* **7**, 703(1961).
22. S. W. Wise *Eclogae Geol. Helv*. **63**, 775-797(1970).
23. M A Cariolou and D E Morse, *J. Comp. Physiol* **B157**, 717-729(1988).
24. S Weiner and W Traub, *FEB Lett* **111**, 311-316(1980).
25. H Nakahara, G Bevelander and M Kakei Haliotis rufescens. *Venus* **41**, 33-46(1982).
26. Y Kitano and D W Hood; *J. Oceanogr. Soc.. JPN* **18**, 35-39(1962).
27. C H Gregoire, *Arch. Int. Physiol. Biochim*. **68**, 836(1960).
28. CH. Gregoire, *J. biophys. Biochem. Cytol*. **9**, 395-400(1960).
29. G Falini, S. Albeck, S. Weiner and L. Addadi; *Science* **271**, 67-69 (1996).
30. R. Naslain, R. Paillar, X. Bourrat, and F. Heurtevent, *Mimicking the layered structure of natural shells as a design approach to fiber matrix interface in Proceed*. *ECCM-8* (J. Girelli – Visconti ed.), Vol.4, Woodhead Publ CMCs,., Abington, Cambridge, UK pp 191-199 (1998).
31. B L Smith, *Chemistry and Industry* **16**, 649-653(1998).
32. Marthe Rousseau, Evelyne Lopez, Alen Coute, Gerard Mascarel, David C Smith and Xarier Boarrat, *9th International Symposium on Biomineralization*, 6-9 December(2005) Pucon, Chile.
33. R.Konwar, R Changmai and G D Baruah; *Indian J. Pure & Appl. Phys*. **42**, 812-815 (2004).
34. A Richard Palmer, "Antisymmetry" in Variation, Hallgrimmson, B and B. K. Hall(eds), *Elsevier*, Chapter 16, (2005) pp 359-397.
35. A H Church, On the Relation of Phyllotaxis to Mechanical Law, (Williams and Norgate, London) 1904.